
FACULTY OF TECHNOLOGY

# VALIDATION OF TORNIO AP3 MODEL BASED FURNACE CONTROL AND GRAIN SIZE CALCULATION

Pekka Hyttinen

MASTER'S PROGRAMME IN MECHANICAL ENGINEERING

Master's Thesis

September 2021

# TIIVISTELMÄ

Tornion HP3-linjan mallipohjaisen uunin ohjauksen ja rakeenkasvun validointi

Pekka Hyttinen

Oulun yliopisto, Konetekniikan maisteriohjelma

Diplomityö 2021, 82 s. + 4 liitettä

Työn ohjaajayliopistolla: Jari Larkiola

Hehkutus- ja peittauslinja 3:n automaatio uusittiin vuonna 2016, mutta uunien mallipohjainen ohjaus ei ollut riittävän hyvällä tasolla, jotta tuotannossa voitaisiin luottaa siihen. Tämän vuoksi mallin validointi oli tarpeellista. Tavoitteena oli saada malli toimimaan siten, että uuneja voitaisiin ohjata pääasiassa pelkästään automaatiolla ilman operaattoreiden panosta.

Raekokolaskennan taustalla olevia ilmiöitä ja automaatiota tarkasteltiin kirjallisuuden pohjalta tietopohjan luomiseksi. Ongelmaa lähestyttiin tarkastelemalla lähdekoodia ohjelmointivirheiden osalta, seuraamalla laskennan lokitietoja, tarkastelemalla automaation käyttämiä taulukoita, hyödyntämällä tilastollista tietoa, sekä vertaamalla laskennan tuloksia tuotantokokeiden tuottamaan raekokoon.

Laskennan tarkkuutta on mahdollista parantaa modifioimalla sekä raekoko-, että vyöhykkeiden asetusarvojen laskentaa. Laskentaan ehdotettiin useita parannuksia yleisiin parametreihin, laatukohtaisiin rakeenkasvuparametreihin ja lähdekoodiin. Näiden parannusten perusteella laskennan suurin virhe on 0,45 ASTM yksikköä. Tuotantolinjan heikon vyöhykelämpötilan hallinnan takia näidenkään muutosten jälkeen tarkkuutta vaativia hehkutuksia ei voida suorittaa. Automaation korjaus on aloitettu, mutta sitä ei ehditty viemään loppuun tämän projektin puitteissa.

*Asiasanat: automaatio, hehkutus, ruostumaton teräs, austeniitti*

# ABSTRACT

Validation of Tornio AP3 model-based furnace control and grain size calculation

Pekka Hyttinen

University of Oulu, Master's Programme in Mechanical Engineering

Master’s thesis 2021, 82 pp. + 4 Appendixes

Supervisor at the university: Jari Larkiola

Automation for annealing and pickling -line 3 was renewed in 2016, but the model-based control wasn’t good enough that production could rely on it, so doing modifications to the model was necessary. The goal was to get the model working so that automation could control furnaces mostly without input from line operators.

Phenomena concerning grain size calculation in the automation system was studied theoretically to acquire sufficient information. The solving of problem was done by inspecting source code for programming errors, examining calculation log files and tables used by automation and finally measuring accuracy of the calculation both statistically and comparing calculated results with measured grain size from production trials.

The accuracy was improved by modifying both grain size calculation and set-point calculation. Many changes were suggested for general parameters, grain specific grain growth parameters and source code. After these changes maximum grain size calculation error improved to 0,45 ASTM, but because of poor control of zone temperatures high accuracy in annealing can’t be done. The fixing of automations system is started, and it continues even when this thesis project is finished.

*Keywords: automation, annealing, stainless steel, austenite*

# FOREWORD

The work for this Master's Thesis was done between 15.3.2021 and 15.9.2021 in Tornio Research Centre of Outokumpu Oy.

I would like to thank Elina Riekki and Outokumpu overall for providing me with the subject, financial support and opportunity to do my Master's Thesis at Outokumpu. It was enjoyable to realize that the summers I have worked here culminated in this project. I would also provide special thanks to Tommi Saatio who acted as my instuctor for this project from Outokumpu and was always willing to give advice and kick me forward if work was not advancing. Also thanks to everyone else at Outokumpu who helped and worked with me for this project.

I would also like to thank University of Oulu and its staff for the quality education is has provided. Special thanks to Jari Larkiola who acted as the instructor from University of Oulu and who was together with Tommi always optimistic about this work even if I personally was not. Also thanks to my fellow students at the university and my family, who kept encouraging me and without whom I propably would have quit studying mechanical engineering and started doing something else.

Tornio, September 2021

*Pekka Hyttinen.*
Pekka Hyttinen

# TABLE OF CONTENTS

# SYMBOLS

| | |
|---|---|
| $A$ | Area |
| $C$ | Specific heat |
| D | Thermal diffusivity |
| $D_M$ | Mean grain size |
| $D_z$ | Grain size limit (Zener) |
| $F_v$ | Volume fraction of particles in Zener pinning |
| $I$ | Intensity |
| $I_b$ | Intensity for black body |
| $I_\lambda$ | Resulting intensity for specific wavelength |
| $I_{\lambda_0}$ | Initial intensity for specific wavelength |
| $K$ | Grain growth parameter |
| $L$ | Length |
| $P$ | Driving pressure for grain growth |
| $P_z$ | Zener pinning pressure |
| $Q$ | Activation energy |
| $\dot{Q}$ | Rate of heat flow |
| $\dot{Q}_g$ | Rate of radiated heat from gas |
| $\dot{Q}_{rad}$ | Rate of radiated heat to strip |
| $\dot{Q}_{con}$ | Rate of radiated heat convectively to strip |
| $\dot{Q}_{adv}$ | Rate of radiated heat using advection to strip |
| $R$ | Universal gas constant |
| $T$ | Absolute temperature |
| $T_{aw}$ | Adiabatic wall temperature |
| $T_g$ | Atmosphere temperature |
| $T_{in}$ | Arriving strip temperature |
| $T_{out}$ | Leaving strip temperature |
| $T_s$ | Radiation source temperature |
| $T_w$ | Surface temperature |
| $T_{log}$ | Logarithmic temperature difference |
| $T_\varepsilon$ | Emissivity temperature level |
| $W$ | Strip width |

| | |
|---|---|
| $a, b, c, n$ | Equation specific coefficient |
| $e$ | Energy flux |
| $d$ | Strip thickness |
| $h$ | Heat transfer coefficient |
| $m_{11}$ | *TempRelationPreHeat11* -parameter |
| $m_{12}$ | *TempRelationPreHeat12* -parameter |
| $p$ | Partial pressure |
| $q$ | Heat flux |
| $q_b$ | Heat flux for black body |
| $r$ | Mean radius of the grain sphere |
| $r_p$ | particle radius |
| $t$ | time |
| $v$ | Velocity |
| | |
| α | Absorptivity |
| $\alpha_g$ | Gas absorptivity |
| γ | Grain boundary energy |
| $\varepsilon$ | Emissivity |
| $\varepsilon'_g$ | Emissivity of gas calculated at surface temperature using modified path length |
| $\varepsilon_z$ | Zone specific emissivity after temperature adjustment |
| $\varepsilon_{z0}$ | Zone specific emissivity from parameter table |
| $\kappa$ | Thermal conductivity |
| | |
| λ | Wavelength |
| $\rho$ | Density |
| σ | Stefan-Boltzmann constant [$5.669\times10^{-8}$ W/(m$^2$·K$^2$)] |

# 1 INTRODUCTION

The automation system of AP3 line in Tornio was completely renewed in 2016. The new automation system delivered by ABB is equipped with a similar model-based furnace control and grain size calculation functionality as the other AP-lines in Tornio. After the revamp, the annealing line has still been operated manually by using preset table temperature values since the furnace control can be trusted to the furnace model only after the correct operation has been verified. Validation of the model-based furnace control and grain size calculation functionality in the new automation system was started previously, but more work is needed for the model to satisfy its full potential.

The calculation model is similar for each annealing and pickling line at Outokumpu Tornio plant, so there was no need to create it from scratch. The theoretical background of the model is introduced. This includes heat transfer, grain growth and recrystallization fundamentals. The annealing and pickling process, modeling of process and controlling the furnace are explained briefly.

The validation process tries to answer the following questions:

- What changes are needed so that set-point calculation will work properly for hot and cold bands at AP3?
- What changes are needed so that grain size calculation will work properly for hot and cold bands at AP3?
- What changes and documentations are needed so that model can be taken in to use at AP3?

Validation starts off with an introduction of automation parameters. Then the grain size calculation and set-point calculation are explained. Parameters are one of the main points of the validation process, and they are resolved based on what other people have determined and how the current parameters and possible alternative parameters work when compared to grain size measurement data from quality control samples. Lastly the set-point calculation is validated using production trial and required changes listed.

When the model-based furnace and grain size control works as expected and is validated, it can be utilized to reduce scrapping, reallocation and rework due to wrong mechanical properties and remaining scale since annealing temperature can be controlled more precisely in the case of speed changes, and variation based on human way of working would be reduced. More accurate furnace control would enable reduction of furnace fuel consumption, which in turn with reduced scrapping, reallocation and rework would reduce $CO_2$ emissions. $CO_2$ emission restrictions will be stricter in the future, and to keep up with the industry improving the annealing process control is a must.

# 2 THEORY

## 2.1 Heat transfer

Temperature changes at strip require heat to transfer to the strip. Outokumpu uses generally the same heat transfer model for each annealing and pickling line. Heat transfer model is based on law of conservation of energy. This means that the heat energy exiting zone via advection is equal to heat energy received from radiation and convection. This balance is nominated by

$$\dot{Q}_{rad} + \dot{Q}_{con} + \dot{Q}_{adv} = 0 \quad (1)$$

where $\dot{Q}_{rad}$is energy transferred by radiation, $\dot{Q}_{con}$ energy transferred by convection and $\dot{Q}_{adv}$ energy transferred by advection. Advection is the heat energy leaving because of the movement of the strip. It is calculated straightforwardly as

$$\dot{Q}_{adv} = \rho\ C\ d\ W\ v\ (T_{in} - T_{out}) \quad (2)$$

where $\rho$ is the density of the material, $C$ is the specific heat of the material, $d$ is the thickness of the strip, W is the width of the strip and v is the velocity of the strip. $T_{in}$ and $T_{out}$ are the temperatures of the strip when arriving at the zone and leaving the zone respectively (Manninen 2020b). Other heat transfer mechanisms are inspected in more detail.

### 2.1.1 Radiation

Thermal radiation is electromagnetic radiation emitted by a body at the expense of its internal energy. Most of thermal radiation have a wavelength from 0,1 to 100 µm, but for practical purposes wavelength range between 0,4 to 15 µm is the most interesting. Photons with corresponding energies can change the vibrational rotational and electronic energy states of atoms and molecules they are influencing, thus changing the internal energy and temperature of material. (Rohsenow et al. 1998 p. 7.2)

All liquids and solids emit thermal radiation, as do some gasses (Rohsenow et al. 1998 p. 1.3). Most solids and liquids are opaque to thermal radiation, meaning energy cannot be transmitted through them as radiation. Many gasses on the other hand are practically transparent to thermal radiation, and energy flux through them is undiminished. Therefore, these gasses can't receive energy through radiation. (Hewitt et al. 1994 p. 120)

An ideal radiator, or better known as blackbody, absorbs all radiation from every wavelength and every direction, blackbody is the best possible emitter in every wavelength and the spectrum of emitted radiation is dependent only on absolute temperature. With such qualities, blackbody is a convenient standard for comparing properties of real materials. (Rohsenow et al. 1998 p. 7.3; Hewitt et al. 1994 p. 120) Blackbody emits an energy flux according to Stefan-Boltzmann law:

$$q_b = \sigma T^4 \tag{3}$$

where $q_b$ is energy flux, $\sigma = 5{,}670\times10^{-8}\frac{W}{m^2K^4}$ is known as Stefan Boltzmann constant and $T$ is absolute temperature. Since emitted radiation increases in proportion to the absolute temperature to the fourth power, radiation tends to be the most significant heat transfer mode in high temperatures. Real world materials don't operate like idealized radiator, so Stefan-Boltzmann law is modified into

$$q = \varepsilon\sigma T^4 \tag{4}$$

ε is known as emissivity, which is a surface property between 0 and 1. Idealized blackbody has emissivity of 1. Emissivity itself is defined as

$$\varepsilon=\frac{I}{I_b} \tag{5}$$

where $I$ is the radiation intensity for the real surface and $I_b$ radiation intensity for the equivalent blackbody. Emissivity is in general dependent on temperature of the emitting surface, wavelength and direction of the radiation. The emissivity used often in engineering applications is called total monochromatic emissivity, where emissivity for specific wavelength is integrated over the whole surface. Integration can also be one over all wavelengths for specific direction (Hewitt et al. 1994, p. 126). Integrating over both wavelength and direction yields hemispherical total emissivity (Rohsenow et al. 1998 p. 7.6)

Absorptivity is the property of the surface that defines the fraction of the energy that is absorbed. Like emissivity, absorptivity is dependent on the direction and wavelength of the radiation, and temperature of the surface. Kirchoff's law states that emissivity and absorptivity are equal if irradiation is associated with a blackbody at the same temperature as the surface

$$\varepsilon = \alpha \tag{6}$$

where α is absorptivity. While Kirchoff's law isn't entirely accurate in practical cases such as annealing line, it is often reasonable enough assumption and using it makes applications simpler. (Hewitt et al. 1994, p. 135)

Furnace atmosphere consists of gasses. As previously mentioned, many gasses are transparent in terms of absorptivity. These gases are nonpolar molecules like oxygen molecule ($O_2$) and nitrogen molecule ($N_2$). Gases like $CO_2$, $H_2O$ and $NH_4$ both absorb and emit radiation. (Hewitt et al. 1994, p. 144).

At a specific wavelength λ, when radiation with intensity $I_{\lambda_0}$ passes through volume of gas, the intensity will be reduced by absorption. The resulting intensity is calculated

$$I_\lambda = I_{\lambda_0} e^{-b_\lambda pL} \tag{7}$$

where $b$ is a coefficient, $p$ is partial pressure and $L$ is the length of which radiation passes. This is also known as Beer's law. Similar relationship applies to emission from gasses. When this is summed over all wavelengths, the total effective absorptivity of gas volume is

$$\alpha_g = \frac{\Sigma_\lambda I_{\lambda_0} e^{-b_\lambda pL}}{\Sigma_\lambda I_{\lambda_0}} \tag{8}$$

In equations (7) and (8) $b$ is highly dependent on temperature, meaning absorptivity of gas is different from emissivity of gas at temperature $T_g$ so Kirchhoff's law was adjusted. An empirical equation taking this into account can be applied (Edwards, 1983)

$$\alpha_g = (\frac{T_g}{T_s})^n \varepsilon'_g \tag{9}$$

where $T_s$ is the temperature of radiation source and $\varepsilon'_g$ is emissivity of gas calculated at surface temperature using modified path length:

$$pL' = pL(\frac{T_w}{T_g}) \tag{10}$$

Index $n$ has value depending on gas. When dealing with surface in enclosure like a furnace, the emission from the gas to the surface is given by

$$\dot{Q}_g = dA\sigma\varepsilon_g T_g^4 \tag{11}$$

where $A$ is the area of the irradiated surface. Heat transfer from gas to surface area unit is

$$q_g = \sigma\varepsilon_g T_g^4 - \sigma\alpha_g T_w^4 \tag{12}$$

assuming surface acts as a blackbody. For grey surfaces the heat flux is reduced by factor $\varepsilon_w$. (Hewitt et al. 1994, p. 145… 147)

Outokumpu uses streamlined version of equation 12 where Kirchhoff's law is more generally applied

$$\dot{Q}_{rad} = 2\,\varepsilon\,\sigma\,L\,W\,\left[T_g^4 - \left(T_g - T_{log}\right)^4\right] \tag{13}$$

where L is the length of the strip within zone, W is the width of the strip and $T_{log}$ logarithmic temperature difference.

### 2.1.2 Convection

Convection is heat transfer mode where heat is transferred across flow plane within flowing fluid. The fluid can be either gas or liquid. Technically the transfer method that happens during convection is conduction. The general process of heat transfer across boundary surface exposed to low-velocity fluid stream can be defined with Newton's law of cooling (Rohsenow et al. 1998, p. 1.54)

$$q = h(T_w - T_g) \tag{14}$$

Where h is heat transfer coefficient, $T_w$ is the surface temperature and $T_g$ is the characteristic fluid temperature. Since $q = \frac{\dot{Q}}{A}$, the heat across known surface q is given by

$$\dot{Q} = Ah(T_w - T_g) \tag{15}$$

where A is surface area. The heat transfer coefficient is dependent on surface geometry, physical properties of the fluid and its velocity. In some situations $h$ can depend on the temperature difference. (Rohsenow et al. 1998, p. 1.4)

Convective heat transfer coefficient is dependent on many factors, so determining it can be rather challenging especially since multiple modes of heat transfer are generally active at once. Since convective heat transfer coefficient is highly dependent on environmental factors, it can be determined experimentally or by doing simulations (Tafreshi et al. 2020). Su (2017) created a fitting equation (16) for coefficient for their three-dimensional mathematical continuous annealing furnace model. They linked coefficient to gas density and velocity:

$$\mathrm{h} = 4{,}04(1 + 1{,}05\rho\mathrm{v}) \qquad (16)$$

If the velocity of the fluid increases, $T_g$ in equation (15) is replaced by $T_{aw}$, or adiabatic wall temperature. Adiabatic wall temperature is defined as

$$T_{aw} = T_g + a\frac{v^2}{2c_p} \qquad (17)$$

where $v$ is the velocity of the fluid and $a$ is dimensionless recovery factor of the fluid. $a$ usually gets values between 0,8 and 1,0. (Rohsenow et al. 1998, p. 1.5)

### 2.1.3 Conduction

When medium is subjected to temperature gradient, heat flows by thermal conduction from higher temperature region to region with lower temperature. In simple, one dimensional case, heat flux caused by this phenomenon is explained by Fourier's law

$$q = \kappa\frac{\Delta T}{L} = -\kappa\frac{dT}{dx} \qquad (18)$$

where heat flux $q$ is heat flux, $\kappa$ is property of the medium known as thermal conductivity, $\Delta T$ the thermal difference between areas and $L$ the distance.

Thermal conductivity depends upon transfer of energy associated with the atoms and molecules of the medium. The transfer mechanism depends on the state of the medium.

In solid matter conduction happens largely through vibrations of the atoms and movement of electrons, but in liquids and especially gasses collision of moving atoms is the main way of transferring energy. Because electrons play a significant part in transferring heat in solids, metals tend to be good heat conductors. Crystalline structure also helps with conductivity. In liquids and gases atoms are further apart, so thermal conductivity is also smaller. (Hewitt et al. 2000, p. 13)

Heat conductivity is almost always affected by temperature. In pure metals conductivity falls as temperature rises, but in some metals or alloys this isn't the case. Notably in stainless steel is exception to this. Liquids tend to become less conductive with temperature, but gases become more conductive due to increased atom velocity. (Hewitt et al. 2000, p. 15)

In a three-dimensional case, when thermal conductivity is constant and there is no internal heat generation the general form of heat conduction is

$$\nabla^2 T = \frac{1}{\mathrm{D}} \frac{\partial T}{\partial t} \tag{19}$$

Where $D = \frac{\kappa}{\rho C}$. It is known as thermal diffusivity, and it describes how fast a temperature change will be diffused through the medium. $C$ is specific heat capacity and $\rho$ is density. (Hewitt et al. 2000, p. 17)

Conduction isn't significant form of heat transfer in furnace atmosphere compared to radiation and convection, but the knowledge of it is needed if the speed which the inner part of heated load reaches the outer parts temperature is of interest. (Kivivuori & Härkönen 2005, p. 125)

### 2.1.4 Logarithmic mean temperature difference

As we have seen, heat exchange rate is often proportional to the temperature difference between two bodies. In real world applications, temperature difference isn't always constant. For example, in annealing furnace, the temperature of the strip arriving to the zone is different from strip leaving the zone. In these situations, temperature difference is

substituted with logarithmic mean temperature difference. Arithmetic mean temperature doesn't give accurate description of the situation, since temperature change isn't linear. This situation has been visualized in figure 1. (Connor 2019)

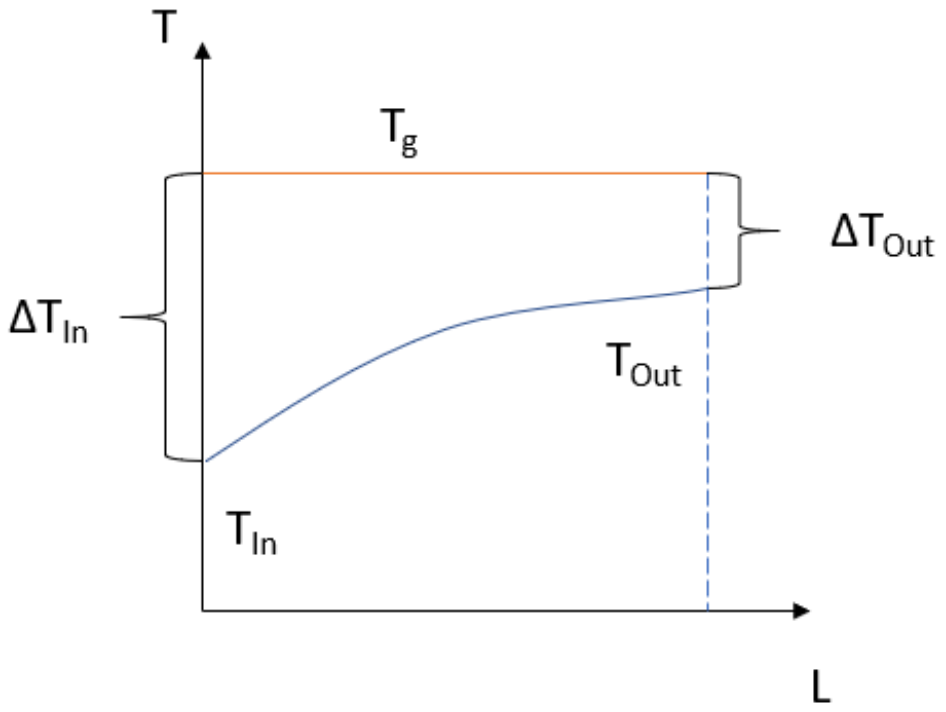


Figure 1. Temperature difference in realistic situation. (Connor 2019, retell)

In a situation where temperature of one of the mediums is basically constant and always higher than temperature of the second medium, like annealing furnace atmosphere, logarithmic mean temperature difference can be explained with equation (20):

$$T_{log} = \frac{T_{out} - T_{in}}{\ln\left(\frac{T_g - T_{in}}{T_g - T_{out}}\right)} \tag{20}$$

where $T_g$ is the temperature of the medium with constant temperature, $T_{out}$ is temperature of medium leaving the zone and $T_{in}$ is the temperature of medium arriving in the zone. (Manninen 2020b)

In a more general situation, where temperature of one of the mediums isn't constant, equation for logarithmic mean temperature difference becomes

$$T_{log} = \frac{\Delta T_{in} - \Delta T_{out}}{\ln\left(\frac{\Delta T_{in}}{\Delta T_{out}}\right)} \quad (21)$$

where $\Delta T_{in}$ and $\Delta T_{out}$ are the temperature differences in entry and exit points of the zone. (Rohsenow et al. 1998, p. 17.32)

## 2.2 Thermal properties of austenitic stainless steels

The thermal conductivity of stainless steels is generally lower than that of carbon steels. For ferritic and martensitic steels thermal conductivity is about 30 W/m °C and for austenitic and duplex steels it is about half that. The thermal conductivity correlates with temperature by increasing a bit as temperature rises. Heat capacity of carbon steel and stainless steel is roughly 500 J/kg °C. (Outokumpu Oyj 2017 s. 55)

As stated in chapter 2.1.1, emissivity is dependent on the temperature. Liu et al. (2013) studied emissivity of three different stainless steel grades. ASTM grades 304 (EN 1.4301), 201 (EN 1.4372) and 321 (EN 1.4541) and their temperature dependencies were studied. Emissivity measurements were made and using linear least-squares technique results were fitted into general function, forming functions (22), (23), and (24) for grades 201, 304 and 321 respectively.

$$\varepsilon_{201}(T) = 0{,}06694 + 0{,}12231 \times ln(T - 741{,}18501) \quad (22)$$

$$\varepsilon_{304}(T) = 0{,}17137 + 0{,}10353 \times ln(T - 744{,}09288) \quad (23)$$

$$\varepsilon_{321}(T) = -0{,}18793 + 0{,}15679 \times ln(T - 726{,}80628) \quad (24)$$

Where $\varepsilon$ is the emissivity of the grade and $T$ is the absolute temperature of the material. These functions are plotted in figure 2. The deformation state or the heat treatment history of the material wasn't published, but the chart shows that titanite stabilized grade 321 has generally lower emissivity than grades 201 and 304.

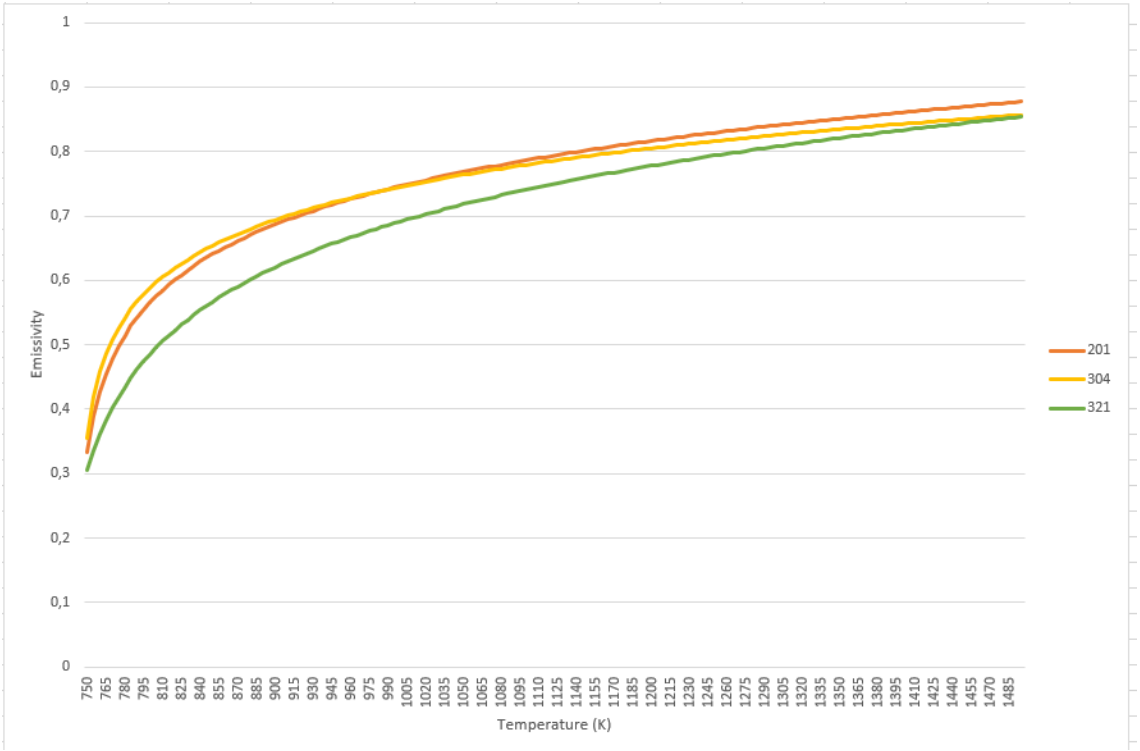


Figure 2. Emissivity of grades 201, 304 and 321 as proposed by Liu et al. (2013).

Zareba et al. (2016) used nonlinear least-squares optimization algorithm to find suitable parameters for their stainless steel annealing furnace model. Their algorithm gave cleaned stainless steel strip emissivity of 0,015995… 0,292523. Due to temperature dependency the emissivity in furnace environment is at lowest around 0,15. In a different study, emissivity of polished stainless steel was measured to be 0,0417 in cryogenic temperature of 80 K (Woods et al. 2014).

## 2.3 Restoration of microstructure

Restoration of the crystalline structure of the deformed metal can happen either through recovery, recrystallization or grain growth. They are all processes that lead to softening, meaning strength of the material falls. These processes exponentially increase in speed as temperature rises, to the point at high temperatures they seem instantaneous. (Ginzburg 2005, p. 313-314)

The rates vary wildly from metal to metal depending on composition, purity, grain size before deformation and amount of deformation. Metals with low melting points tend to show higher rates at lower temperatures. Sometimes the three processes can occur simultaneously, sometimes they are clearly separated. (Ginzburg 2005, p. 315)

Driving force behind restoration of microstructure is internal energy of the material. Microstructure aims to minimize this internal energy stored in grain boundaries, point defects and dislocations, resulting in effects such as recrystallization, recovery and grain growth. Microstructures are generally metastable, meaning energy from outside is needed to start these effects.

### 2.3.1 Recrystallization

Primary recrystallization involves the formation of new strain-free grains in the material consuming deformed and recovered microstructure in the process. Microstructure at any point can be divided into recrystallized or non-recrystallized region. Exaggerated grain growth in fully recrystallized material is sometimes called secondary recrystallization or abnormal grain growth (Humphrey and Hatherly 1995, p. 173). Primary recrystallization will be referred simply as recrystallization and secondary recrystallization as abnormal grain growth in the future.

Mehl (1948), Burke and Turnbull (1952) (according to Humphrey and Hatherly 1995, p. 177) defined laws of recrystallization. The laws of recrystallization are set of rules recrystallization process usually obeys. The main idea behind these rules is that the driving force behind the process is provided by stored energy provided by the deformation. The laws are as follows:

- A minimum deformation is needed to initiate recrystallization
- The recrystallization temperature decreases as annealing time increases
- The recrystallization temperature decreases as strain increases
- Recrystallized grain size depends primarily on amount of deformation, larger deformation resulting in smaller grain size
- Recrystallization temperature increases with pre-recrystallization grain size and deformation temperature

These laws were discovered in 1952 and considering modern knowledge they are considered imperfect and hard to extrapolate. They still provide useful guide to overall behavior of material.

Most commercially used metals and alloys contain more than one phase. Often this is in form of dispersed particles. These particles increase stored energy, may act as nucleation sites for recrystallization and closely spaced particles may exert pinning effect to grain boundaries. The first two effects promote recrystallization while the last one hinders it. Compared to single-phase alloys, recrystallization is inhibited by closely spaced particles, showing pinning effect is very significant compared to the other two effects. Since the size, distribution and volume of second-phase particles are affected by composition and thermomechanical processing, they can be used control microstructure and texture of alloys. (Humphreys and Hatherly 1995, p. 235, 256)

The texture formed during recrystallization is of great interest, because texture is largely used to explain directionality of properties in finished product. It is worth mentioning that initial texture has effect on recrystallized texture, recrystallization texture changes during grain growth and that impurities can greatly affect recrystallization texture. (Humphreys and Hatherly 1995, p. 327)

### 2.3.2 Recovery

Recovery and recrystallization are competing processes, since both use the internal energy of deformed material and once recrystallization has consumed deformed microstructure, no further recovery can happen. Recovery isn't a single microstructural process, but rather refers to the changes in the properties of a deformed material, which occur before recrystallization. The primary factor of recovery are the changes to the dislocation structure. Dislocations rearrange and annihilate. (Humphreys and Hatherly 1995, p. 127, 135)

### 2.3.3 Grain growth

The grain size model in use at Outokumpu uses theory originally by Burke and Turnbull. This model assumes that the driving pressure P on a boundary arises only from the curvature of the boundary.

$$P = \frac{a\gamma}{r} \tag{25}$$

Where γ is the energy of the boundary, $a$ is a small geometric constant and r is the mean radius of the sphere. The model assumes that γ is the same for all boundaries. The theory further assumes that boundary velocity is proportional to the driving pressure, and giving

$$\frac{dr}{dt} = \frac{ac\gamma}{r} \tag{26}$$

Integrating equation (26) gives us

$$r^2 - r_0^2 = 2ac\gamma t = Kt \tag{27}$$

Where $r_0$ is the initial mean grain size, $c$ is a constant and $K$ is the combined factor, that is dependent on material in question and temperature. The temperature dependency of $K$ can be expressed as

$$K = K_0 e^{-\frac{Q}{RT}} \tag{28}$$

where $K_0$ and activation energy $Q$ are material constants, $R = 8{,}314\ \frac{J}{K\ mol}$ also known as the universal gas constant and $T$ is the absolute temperature. Through experimentations it was discovered that grain growth exponent isn't always 2. Thus equation (28) can be written in more general from as

$$r^n - r_0^n = Kt \tag{29}$$

where $n$ is the grain growth exponent. (Humphreys and Hatherly 1995, p. 284)

Grain size model used at Outokumpu uses a modified version of previous equation (29) as seen in equation (30), where grain growth exponent is reciprocal and $K$ receives the same grain growth exponent. All grain growth parameters in the grain growth model are defined for this equation. (Jaiswal et al. 1996, p. 6)

$$r^{1/n} - r_0^{1/n} = K^{1/n}t \tag{30}$$

Which can also be written as

$$r = \left(r_0^{1/n} + K^{1/n}t\right)^n \tag{31}$$

Grain size isn't uniform but rather follows some sort of distribution. Rayleigh distribution has been the most consistent with experimental data. Rayleigh distribution for grain size can be expressed as

$$f(r) = are^{-br^2} \tag{32}$$

where $a$ and $b$ are constant and R is the mean grain size. (Humphreys and Hatherly 1995, p. 298)

As with recrystallization, second-phase particles exert pinning effect on the grain boundaries. The pinning effect acts as a resisting force against driving pressure mentioned in the previous theory. This pinning pressure is known as Zener pinning, and it can be expressed as

$$P_z = \frac{3F_v\gamma}{2r_p} \tag{33}$$

where γ is the boundary energy, $r_p$ is the particle radius and $F_v$ is the volume fraction of said particles. Zener pinning effect gives the grain size limit $D_z$ as seen in equation (34):

$$D_z = \frac{4r_p}{3F_v} \tag{34}$$

Naturally Zener pinning effect requires that precipitation particles are stable. Second phase precipitates begin to coarsen and even dissolve into the matrix in higher temperatures. This can be seen as one of the main reasons why grain growth accelerates in higher temperatures. Liu et al. (2019) for example followed the volume fraction of second phase particles consisting of titanium carbides, nitrides and carbonitrides and found out that volume fraction starts to rapidly drop when reheating temperature passed 1400K. Resulting grain size followed the similar trend. Grain size rapidly grew once reheating temperature passed 1425 K.

### 2.3.4 Abnormal grain growth

During abnormal grain growth, few grains grow excessively consuming the smaller recrystallized grains. This may lead to grain diameter of several millimeters. Avoiding this phenomenon is important part of grain size control. (Humphreys and Hatherly 1995, p. 315)

Abnormal grain growth will not occur in so called “ideal grain array” where there are no impurities and grain boundary energy is constant, since under normal conditions very large grain will always grow more slowly than average grain. It can however occur in situations where normal grain growth is somehow inhibited. (Humphreys and Hatherly 1995, p. 316)

Abnormal grain growth, and grain growth in general can be associated with particles and their pinning effect. The condition in which very large grain will grow is

$$D_M \leq \frac{2r_p}{F_v} \tag{35}$$

where $D_M$ is the mean grain size of grains whose growth has stagnated due to particle pinning, r is the radius of particles and $F_v$ is the volume fraction of particles. (Humphreys and Hatherly 1995, p. 317)

Abnormal grain growth isn't always the serious problem it may seem if only particle limited grain size is considered. Resulting grain size after primary recrystallization may be higher than particle limited grain size, and abnormal grain growth isn't then possible or occurrence of abnormal grain growth is limited by nucleation rather than growth. (Humphreys and Hatherly 1995, p. 319)

Austenitic stainless steels are vulnerable to abnormal grain growth in specific temperatures. In 304L (EN 1.4306) it was noticed to happen in 850 °C… 900 °C and when temperature exceeded 1100 °C. The annealing times used in this study (Shirdel et al. 2014) were very long compared to normal annealing times used in annealing furnaces, and even at 900 °C grain growth was normal for the first 15 minutes.

Padilha et al. (1999) studied the precipitation, grain growth and abnormal grain growth in titanium stabilized EN 1.4970 steel and concluded that grain growth isn't possible in this specific steel in temperatures under 1050 °C. Above this temperature $Cr_2B$ and $Fe_2B$ precipitates dissolve and carbides TiC and MoC dissolve partially. They concluded that between 1050 °C and 1250 °C abnormal grain growth can occur. Their reasoning for this temperature range was that when pinning force is somehow lowered, some boundaries can break away before others and abnormal grain growth occurs. In addition real particle dispersion isn't uniform, but instead consists of particles of different sizes that have different interparticle distances. Above 1250 °C normal grain growth will still occur, but conditions for abnormal grain growth aren't there anymore.

### 2.3.5 Annealing of hot rolled austenitic stainless steel

When steel solidifies, dendrites are formed when temperature drops below liquidus. These may be either austenite or ferrite. For some compositions there may even be both phases solidifying directly from melt. This can solidification known as peritectic solidification can be favorable because ferrite has high solubility for impurities and can therefore counteract hot cracking. (Outokumpu Oyj 2017, p. 21)

Hot rolling is a process that occurs above the recrystallization temperature of the material. Hot rolling process generally begins when temperature of the steel is less than 1315 °C and ends around critical $A_3$ -temperature (Ginzburg 2005, p. 197). Usually the starting material is semi-finished casting product, such as slab, bloom or billet. The cast microstructure is broken down and deformed. The deformed grains recrystallize forming equiaxed microstructure. Hot rolling process flow chart for hot rolling at Outokumpu is shown in figure 3. As can be seen from the chart and as told in Handbook of stainless steel (2017), the milling itself is done using roughing mill, Steckel mill and tandem mill. (Outokumpu Oyj 2017, p. 26-27)

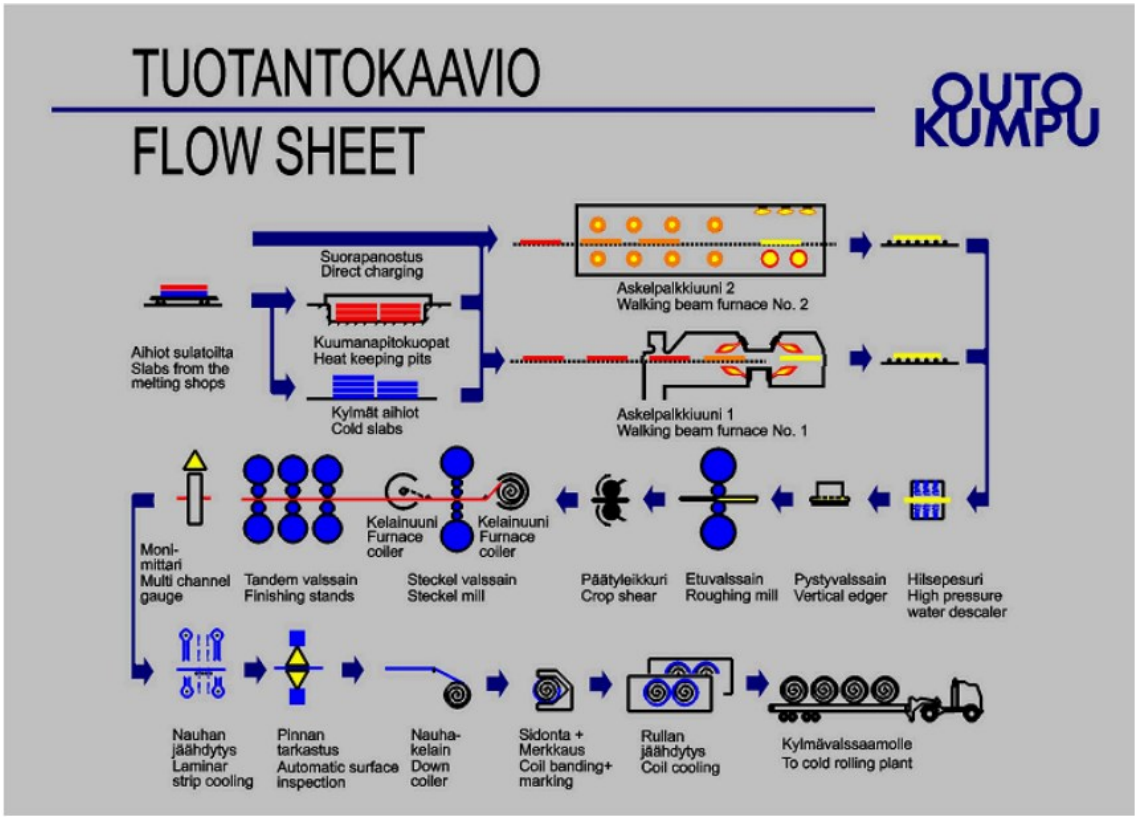


Figure 3. Hot rolling process flow sheet. (Outokumpu)

Restoration during hot rolling happens with dynamic, metadynamic and static processes. Dynamic restoration happens during deformation, metadynamic starts during deformation and completes after deformation while static restoration process starts and completes after deformation. The microstructure formed during dynamic and metadynamic restoration aren't stable and are further modified by static restoration processes. (Ginzburg 2005, p. 317… 325)

Parameters and their effects affecting grain size of dynamic, metadynamic and static recrystallization are introduced in table 1. Static recrystallization happens after dynamic and metadynamic recrystallization and thus dynamically and metadynamically recrystallized grain size affects static recrystallization.

| | Influencing parameter | | | |
|---|---|---|---|---|
| Affected parameter | Temperature | Initial grain size | Strain | Strain rate |
| Dynamically recrystallized grain size | Increases | No effect | No effect | Decreases |
| Metadynamically recrystallized grain size | Increases | No effect | No effect | Decreases |
| Statically recrystallized grain size | Increases or no effect | Increases | Increases | Decreases or no effect |

Table 1. Summary of effects of parameters on final grain size of different recrystallization processes. (Ginzburg 2005, p. 331)

The resulting microstructure differs from cold rolled one quite significantly. Due to the recrystallized microstructure The final grain size after hot rolling is dependent on the reduction of final pass. As expected, larger reduction causes smaller grain size. Thinner strips have larger reduction during final strip, causing them to have smaller grain size going into annealing. This is demonstrated in figure 4. (Tikkanen 2015)

Tikkanen (2015) noted correlation in her report between temperature of the final pass and post anneal grain size. The correlation is strong enough, that the winding temperature can be said to be one the main factors of post anneal grain size. The relationship can be seen in figure 5. In both ends the grain size ends up smaller due to lower temperature.

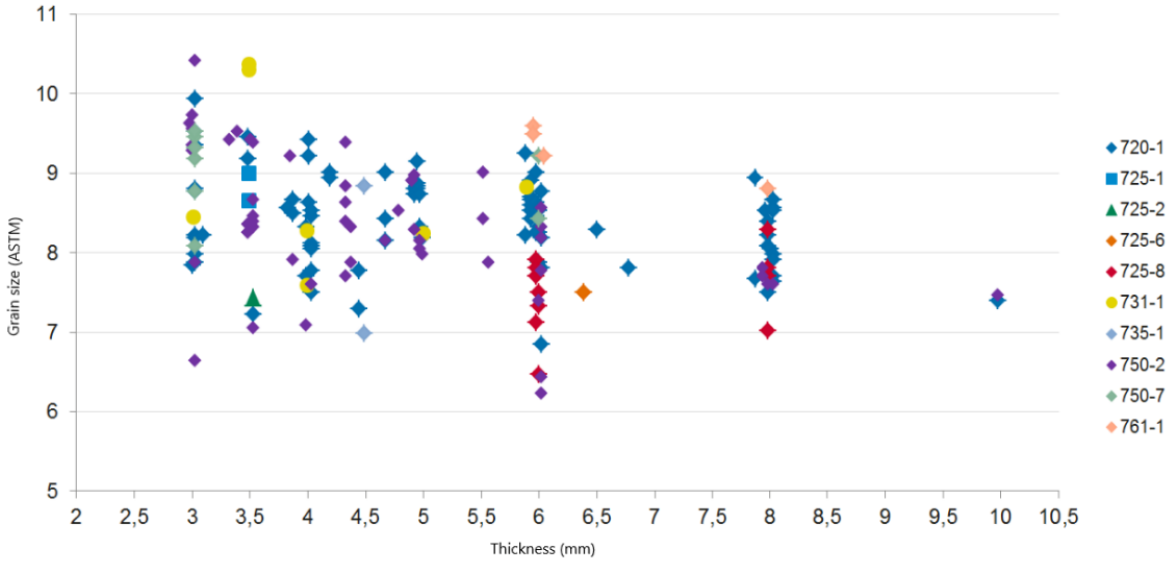


Figure 4. Thickness and grain size correlation (Tikkanen 2015, modified)

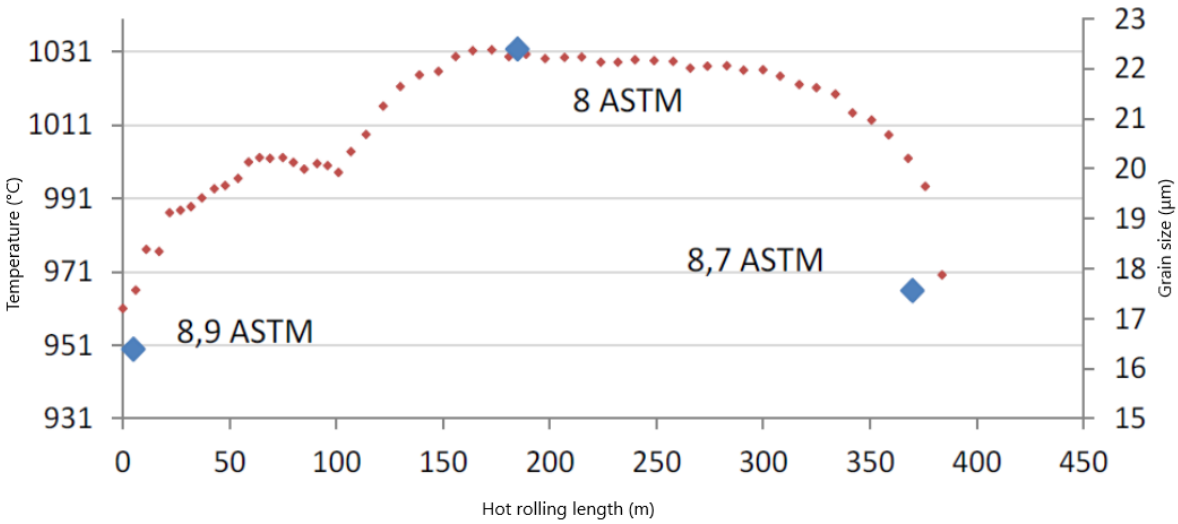


Figure 5. Temperature and grain size correlation (Tikkanen 2015, modified)

Another factor of annealing hot rolled material is the oxidized surface scale that forms during hot rolling. Multi-pass hot rolling of austenitic stainless steel forms a thick and complex surface structure mainly formed of $Cr_2O_3$ and $FeCr_2O_4$ oxides (Cobo et al. 2008). It is well known that the surface condition is one of the main factors of emissivity. Emissivity of stainless steel discussed in 2.2 is mostly applicable to clean surfaces meaning a strip that has gone through pickling process. The annealing furnace comes before the pickling process in the annealing and pickling line, meaning the first annealing is done to a strip covered in surface scale.

The emissivity of oxidized surface varies depending on the steel grade. In experiments done by Liu et al. (2013) to AISI 201, 304 and 321 the emissivity of surface increased by 0,01… 0,06 when isothermal heat treatment in 900 K was applied. In case of carbon steels, oxidization of the surface increased the emissivity from 0,17 all the way up to 0,78. According to Gardner and Ng (2006), emissivity of dull, oxidized surface approaches 1 for stainless steels. Temperature will have some effect on the emissivity for oxidized surfaces, but the effect isn't too significant and can be usually ignored (Švantner et al. 2013).

### 2.3.6 Annealing of cold rolled austenitic stainless steel

As previously mentioned, recrystallization relies on stored energy in the material. Only very small amount, around 1 %, of the energy used in deformation is stored in the material. Rest is released as heat. The stored energy is derived from dislocations and point defects, dislocations being greater contributor to the point that point defects such as vacancies and interstitials are mostly irrelevant when it comes to internal energy. (Humphrey and Hatherly 1995, p. 12)

Cold rolled steel naturally has lower recrystallization temperature due to increased amount of stored energy and larger deformation. It is worth noting that inhomogeneous microstructure leads to non-random distribution of nucleation sites and stored energy and to a growth rate which decreases with time. (Humphreys and Hatherly 1995, p. 203)

As mentioned previously, the emissivity of cold rolled stainless steel is significantly lower than that of oxidized, hot rolled steel. This means that annealing requires more time to reach the same temperature as oxidized steel at the same temperature since transfer of heat energy is slower. Some ways to determine emissivity were given in 2.2, but in the end every model is different and due to simplifications done to the model require their own emissivity parameters. Hewitt et al. (1994, p. 129) give light silvery rough surfaced austenitic stainless steel emissivity value of 0,44.

# 3 MODELING

## 3.1 Measuring furnace temperature

Model-based control is important because accurate, real-time measurement of temperatures is difficult. Design of annealing cycles by plant experimentation are expensive, time consuming and often ineffective. For this reason, mathematical modelling of the process is preferred. There are multiple ways to measure high temperatures, but for different reasons they can't be used to directly measure temperature of the strip inside the furnace. Usually the temperature of the strip is only measured once it exits the furnace using pyrometer, but it is known to have inaccuracies (Zareba et al. 2016).

### 3.1.1 Thermocouple

Thermocouple is a way to electrically measure temperature. Its operation is based on Seebeck-phenomenon. Voltage difference is built between two different metallic wires when their connection point is heated. This voltage increases with increasing temperature difference between hot measuring end and cold reference end. The voltage difference between the ends depends on the metals used in wires in addition to temperature. (Järviluoma and Koskinen 2000, p. 12)

In theory, thermocouple can be made of any electricity conducting material, but in practice pure metals or homogenous alloys are good fit. The materials used in thermocouples can be divided into noble and ignoble metals. Thermocouples made of noble metals are typically different alloys of platinum and rhodium, while ignoble metals are made of copper, constantan, iron and CrNi. Noble metals sport significantly higher temperature resistance, oxidization resistance and purity and thus better accuracy. (Järviluoma and Koskinen 2000, p. 12)

Thermocouples have couple of limitations. Accurate measurements require expensive amplifiers and thermocouples are affected by heat noise. Thermocouples become less accurate with age due to drift, corrosion and generally anything that can affect the

homogeneity of the material. Effect of external heat must be eliminated on the reference point, meaning the reference point must be far enough from heat sources and protected from radiation. Homogeneity of the material can be restored with annealing, but often removing the thermocouple isn't practical. (Järviluoma and Koskinen 2000, p. 16; Webster and Saunders 2020)

### 3.1.2 Pyrometer

Pyrometer measures temperature using radiation emitted by the inspected object. To transform measured radiation into temperature measurement the emissivity of the object is needed. Pyrometer can either measure radiation from all wavelengths or just part of them. Pyrometer that measures only limited wavelengths has generally smaller error compared to pyrometer that measures all wavelengths, since they are less vulnerable to radiation interference. Pyrometer can also use two wavelengths that are close to each other and compare their intensity giving temperature. (Järviluoma and Koskinen 2000, p. 17… 19)

While pyrometer can be used to directly measure the temperature of the object, there are still some problems. Surface emissivity is required, and it can be affected by surfaces environment, wavelength and inspection angle. Water vapor, particles and $CO_2$ in the furnace atmosphere can warp the measurement result and radiation sources outside the inspected object can cause errors. (Järviluoma and Koskinen 2000, p. 19)

## 3.2 Examples of annealing furnace models

One way of identifying parameters is looking into past studies and either creating a equation or directly implementing the equation from a study. This is applied to properties like heat capacity, density, emissivity and flue-gas properties. These equations might include values that aren't directly measurable, so a different method is needed to identify those. Fitting values into these equations can happen through an algorithm, where large

set of data is loaded into the system and values are fitted into the equation. (Zareba et al. 2016)

Prieto et al. (2005) studied the modeling of carbon steel in annealing furnace by varying different values involved in the calculations such as density, emissivity and specific heat capacity. They also varied dimensions and velocity of the annealed strip. Their calculations indicate that only small part of the energy is absorbed by the walls in annealing furnace, and over 98 % is absorbed by the strip. This noticed that inaccuracies in emissivity are less significant than those in density and heat capacity when it comes to the accuracy final temperature of the strip with their model despite being important when it comes to the heat transfer rate distribution. Calculating density of the material is relatively simple but getting accurate estimation of heat capacity can be trickier. Thus, attention should be placed on this property to get good estimation for the model. 10 % change in accuracy of dimensions effects the final calculated temperature in a similar way as density and should be kept accurate.

In an earlier example Yoshitani (1993) divided their model into auxiliary static and the main dynamic model. The dynamic model described the relationship between strip temperature and fuel flow rate including strip dimension changes and velocity changes. The static model assumes instead that fuel flow rate, dimensions and speed remain constant. Parameters were recursively estimated on-line. Yoshitani remarks that recursive estimation is useful for both accuracy and reducing workload of engineers from identification work.

Manninen (2020a) predicted post annealing grain size of hot rolled Outokumpu Supra 316plus (EN 1.4420) with decent accuracy using model used in RAP5. The difference to cold rolled coils was higher starting grain size. The standard error in the grain diameter was 2,4 μm. This indicates that similar model at AP3 line should be sufficiently accurate for hot rolled strip.

# 4 ANNEALING AND PICKLING PROCESS

After hot rolling, the strip is taken to annealing and pickling line in cold rolling mill. Annealing and pickling lines in Tornio are continuous annealing lines, meaning strips are welded together. Annealing and pickling process generally composes of annealing, cooling, pickling washing and depending on the line in question, shot peening. In addition, grease is washed off before the process and the surface quality is inspected after the process. Extensions are welded to every second strip at preparation line exceeding thickness of 3,5 mm to increase yield. Process for annealing and pickling line 3 has been illustrated in figure 6.

While prerequisite to handle cold rolled materials exist, all material processed at AP3 is currently hot rolled. Cold rolled material is directed to other lines. Current state of model-based control doesn't allow cold rolled material to be handled. According to technical specifications, AP3 can handle coils with thickness from 1,5 mm to 10,0 mm, weight from 4800 kg to 28000 kg, width 800 mm to 1650 mm. (Outokumpu 2015)

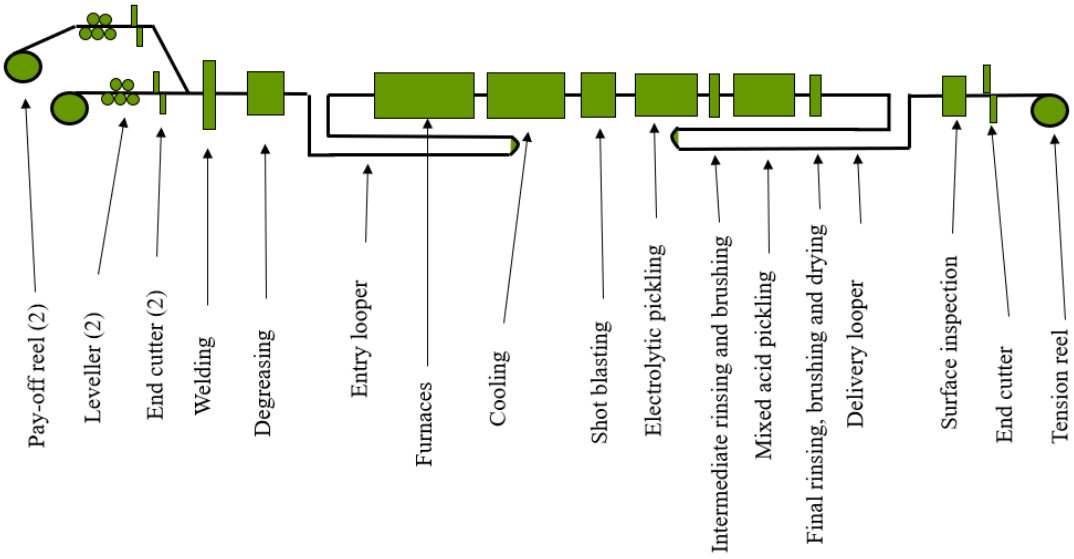


Figure 6. Annealing- and pickling line parts (Outokumpu 2021, modified)

## 4.1 System description

System is divided into three levels. Level 1 is automation and it's handled by control system 800xA by ABB. 800xA is described by ABB as a "comprehensive process automation system". According to ABB (2014) 800xA includes "all automation functions in a single operations and engineering environment; enabling process plants to perform smarter and better at substantial cost savings".

The furnace and grain size model calculations happen at level 2, or L2 in short. L2-system works between automation (L1) and RETU (L3) as a message intermediate while making calculations and saving information. Communication can be divided into event-based coil information transfers and length-based information transfer from automation. (Uusitalo)

Event based transfer flowchart has been visualized in figure 7. In event-based exchange L2 gets information about coil swap from L1 and makes coil information request from RETU. Based on this coil information L2 searches parameters and makes its calculations. Process parameters are then sent to L1. These process parameters are temperature set-points and process line speed. L1 adjusts temperature by controlling the air and gas flow inside the furnace.

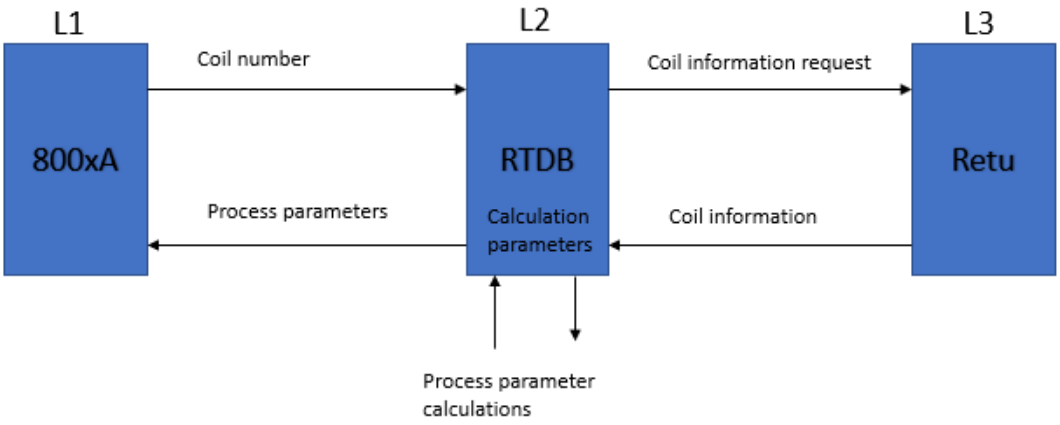


Figure 7. Request chart for event-based transfers.

## 4.2 Furnaces

AP3 line consists of three furnaces. The pre-heating furnace is different from the other two furnaces because it is not directly heated by burning fuel, but rather with flue gasses. This results in a situation where the pre-heat furnace temperature can't be accurately controlled, and its temperature can fluctuate rather significantly.

The control of the furnace is divided into seven different zones. Zones 1 and 2 are for pre-heat furnace, zones 3 and 4 are for furnace 1 and zones 5, 6 and 7 are for furnace 2. Each zone separated in automation in terms of monitoring and control. The numbering changes based on context. In source code the numbering starts from 0, while in some cases pre-heating furnace isn't taken into account and first zone of furnace 1 is called zone 1. Pre-heat furnace is divided into two zones, but currently only one temperature is measured meaning both zones have the same temperature. Explanations and true lengths are shown in table 2.

| Zone number | Zone number (code) | Explanation | Zone length (m) |
|---|---|---|---|
| 1 | 0 | Pre-heat first half | 15,5 |
| 2 | 1 | Pre-heat second half | 15,5 |
| 3 | 2 | Furnace 1 first zone | 11,5 |
| 4 | 3 | Furnace 1 second zone | 11 |
| 5 | 4 | Furnace 2 first zone | 9,15 |
| 6 | 5 | Furnace 2 second zone | 6,9 |
| 7 | 6 | Furnace 2 third zone | 10,15 |

Table 2. Zone numbering.

## 4.3 Pyrometer and thermocouple calibration at Outokumpu

Calibration program contains control devices: sensors, transmitter and amplifiers. Atmosphere temperature is measured with type S thermocouples. Calibration happens every 12 months. An acceptable calibration requires the error between thermocouple and temperature source to be under 4,2 °C. The temperature measurement points are 900 °C, 1000 °C and 1200 °C.

Pyrometers are used to measure the coil temperature. The acceptable calibration error is 10 °C. The pyrometer measurement range is 550 °C… 1500 °C and the measurement points during calibration are 900 °C, 1000 °C, 1100 °C and 1200 °C.

# 5 VALIDATION OF TORNIO AP3 MODEL-BASED FURNACE CONTROL AND GRAIN SIZE CALCULATION

A properly working mode-based furnace control is an attractive proposition, because it could be used to reduce scrapping, reallocation and rework due to wrong mechanical properties. More precise control would enable reduction in furnace fuel consumption. In addition to economic benefit, this would reduce $CO_2$ emissions which is a large advantage in a more climate conscious world.

The original planned phases of original AP3 model validation project are described in table 3. Phases 1 and 2 were considered practically finished before this Master's thesis work, this work is continuation of the original project. In addition to getting AP3 model-based control working properly, project deliverables included description of grain size calculation and furnace control models, proposals how to scale heat transfer parameters form line to line and proposals how to further utilize the model to reduce wrong mechanical properties and furnace fuel consumption. This project concerns only AP3 line, and only austenitic grades.

| Phase | Module / functionality | Feature to be validated |
|---|---|---|
| 1 | Grain size prediction after the annealing. | Heat transfer and grain growth calculations are performed correctly. |
| 2 | Grain size prediction after the annealing. | Input values passed to the grain size prediction module are correct. The input values are the coil properties such as thickness and steel grade and process data such as line speed and furnace zone temperatures. |
| 3 | Heat transfer model parameters characteristic for the AP3 furnace. | Parameters used in the heat transfer model are tested and adjusted if necessary using measured strip temperature data and values calculated by the grain size prediction module. |
| 4 | Model-based control of furnace. | The correct operation of the model-based control is verified by comparing the grain size target and the grain size predicted with the same line speed and using the set-point values as furnace temperatures. |
| 5 | Experimental validation. | Validation of line performance by comparing the produced grain size, the grain size target and the predicted grain size |

Table 3. Project stages.

## 5.1 Parameters for the gain size calculation

As mentioned in 4.1, L2 uses coil number to receive information from RETU, and with line data and parameters from tables L2 does calculations. Grain size model first fetches initial default parameters. These parameters contain initial values for temperature, grain size and things like maximum allowed change with each iteration and furnace zone lengths. There is a large amount of variables, but relevant ones with explanations is presented in appendix 1.

FURNACEMODELGRADECOEFFS table gives us grain size model coefficients n, Q and A. They are fetched based on full Polarit grade and surface code. They match variables $n$, $Q$ and $K_0$ given in equations 27… 31. The parameters describing the kinetics of grain growth are determined with laboratory test. Test material is heat-treated using different heat cycles and final grain size is measured with optical microscope. The non-linear least squares method is then used to identify the unknown parameters. Changes that are sometimes made at Outokumpu to material composition can naturally affect the grain growth kinetics, so systematic issues with grain size prediction are being monitored. (Manninen 2020a)

FURNACETUNING -table holds variables such as emissivity and convection coefficients for each zone, and they are fetched based on the main steel grade, surface code, thickness and width. Parameters with explanations are presented in table 4.

| Variable | Explanation |
|---|---|
| emissivity[0] | Emissivity of the strip in pre-heat zone 1 |
| emissivity[1] | Emissivity of the strip in pre-heat zone 2 |
| emissivity[2] | Emissivity of the strip in zone 1 |
| emissivity[3] | Emissivity of the strip in zone 2 |
| emissivity[4] | Emissivity of the strip in zone 3 |
| emissivity[5] | Emissivity of the strip in zone 4 |
| emissivity[6] | Emissivity of the strip in zone 5 |
| convection[0] | Convection coefficient in pre-heat zone 1 |
| convection[1] | Convection coefficient in pre-heat zone 2 |
| convection[2] | Convection coefficient in zone 1 |
| convection[3] | Convection coefficient in zone 2 |
| convection[4] | Convection coefficient in zone 3 |
| convection[5] | Convection coefficient in zone 4 |
| convection[6] | Convection coefficient in zone 5 |

Table 4. Variables from FURNACETUNINGTABLE

The data provided in table 5 should be provided by RETU. This data is information received during previous work stage.

| Value | Explanation |
|---|---|
| thickness | Strip thickness for coil |
| width | Strip width for coil |
| origthickness | Original strip thickness before cold rolling for coil |
| grade | Steel grade for coil. If missing, model uses default from PARAMETERS -table |
| surfacecode | Surface code for coil. Implies if coil is hot or cold rolled. If missing, model uses default from PARAMTERS -table |

Table 5. Variables received from RETU

Data provided in table 6 is measured at AP3 line during the process. *Pyro_temps* -appear here. and based on logging data *pyro_temps[0]* and *pyro_temps[1]* is a saved zone temperature value that updates periodically. There is an option in code to use average of *pyro_temps[0]* and *pyro_temps[1]* as final coil temperature. Values for *roof_temps* and *zone_temps* are the same, but *roof_temps* have some double values. Other *roof_temps* aren't really used for anything, but due to messy code they exist.

| Value | Explanation |
|---|---|
| roof_temps[0] | Roof temperature zone 1/ Roof temperature pre-heat zone 1 |
| roof_temps[1] | Roof temperature zone 2/ Roof temperature pre-heat zone 2 |
| roof_temps[2] | Roof temperature zone 3/ Roof temperature zone 1 |
| roof_temps[3] | Roof temperature zone 4/ Roof temperature zone 2 |
| roof_temps[4] | Roof temperature zone 5/ Roof temperature zone 3 |
| roof_temps[5] | -/Roof temperature zone 4 |
| roof_temps[6] | -/Roof temperature zone 5 |
| linespeed[0] | Speed at preheat |
| linespeed[1] | Speed at preheat |
| linespeed[2] | Speed at zone 1 |
| linespeed[3] | Speed at zone 2 |
| linespeed[4] | Speed at zone 3 |
| linespeed[5] | Speed at zone 4 |
| linespeed[6] | Speed at zone 5 |
| zone_temps[0] | Temperature of preheat |
| zone_temps[1] | Temperature of preheat |
| zone_temps[2] | Temperature of zone 1 |
| zone_temps[3] | Temperature of zone 2 |
| zone_temps[4] | Temperature of zone 3 |
| zone_temps[5] | Temperature of zone 4 |
| zone_temps[6] | Temperature of zone 5 |
| pyro_temps[0] | - |
| pyro_temps[1] | - |
| length | Strip position (m) for calculation |

Table 6. Measured variables.

## 5.2 Furnace- and grain size model

While parameter tables and the criteria how values are retrieved from them are documented, documentation on how the calculation itself should work is rather lacking. Currently the only extensive documentation regarding model-based furnace control was made by Manninen (2020b) regarding RAP5 production line. As he states in this document, while the underlying principles are similar between all the lines that use model-based furnace control, there are differences in programming language, parameter tables, and whether set-point calculation is event based or cyclical.

The source code for the AP3 model is written in C#. C# is an object-oriented programming language which has its roots in C family (Microsoft 2021). Basically this means that the source code is separated into classes. Most relevant for inspecting the model is FurnaceModel -class which entails the heat transfer calculations and grain size calculations. FurnaceModel -class exists for both grain size and set-point calculations.

### 5.2.1 Grain size calculation

Grain size calculation uses realized zone temperatures to calculate the resulting grain size. It takes the line information, general parameters and coil number which is then used to retrieve the grade and physical dimensions of coil from RETU. This data is used to retrieve the thickness and grade sensitive parameters from parameter table. This is flow is visualized in figure 8.

Originally the model should have been able to use historical information. Idea was that when the strip comes to a specific point outside the furnace, automation calculates positions and times for this specific spot based on line speed and reads matching temperature from history data. The results of calculations are grain size, temperatures at the end of each section, speed of line and error code. That doesn’t happen, but instead only current values are used. Reason for this wasn’t discovered, and ABB was asked to look into this matter.

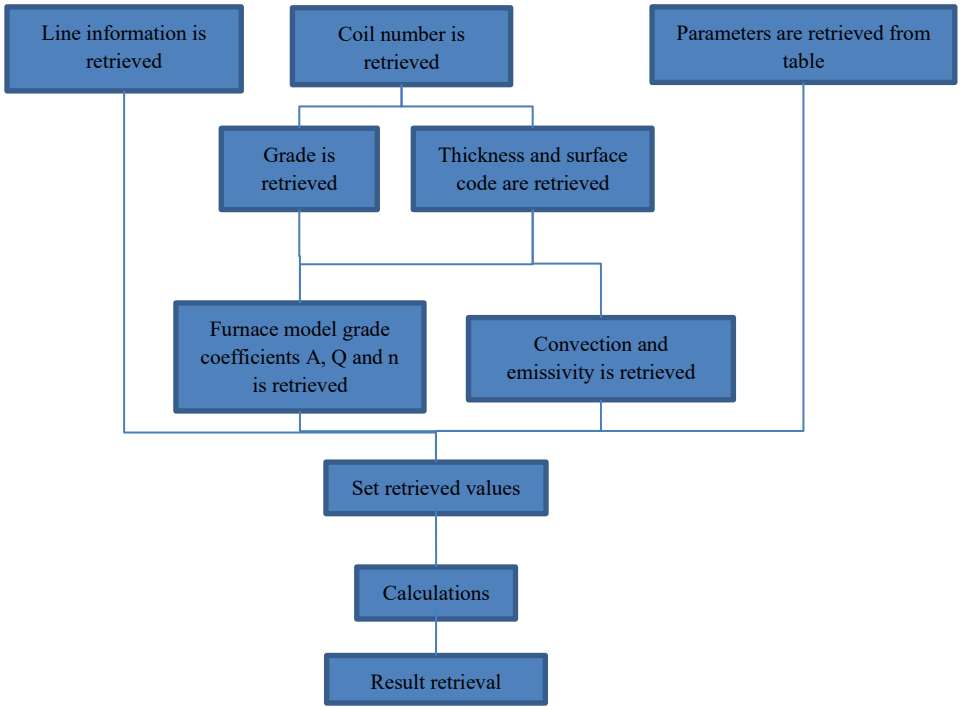


Figure 8. Grain size calculation flowchart.

### 5.2.2 Set-point calculation

Set-point calculation is sometimes refenced as pre-calculation because it calculates results before the annealing happens. What happens during dynamic set-point calculations is that the calculations have a target grain size, and the system calculates zone temperatures which results in the target grain size with the actual line speed. This is visualized in figure 9. As the logic is largely the same as in grain size calculation, but the difference is what is calculated and what values are needed in calculations. There is also an option to use static calculation, where set-points are calculated using nominal speed.

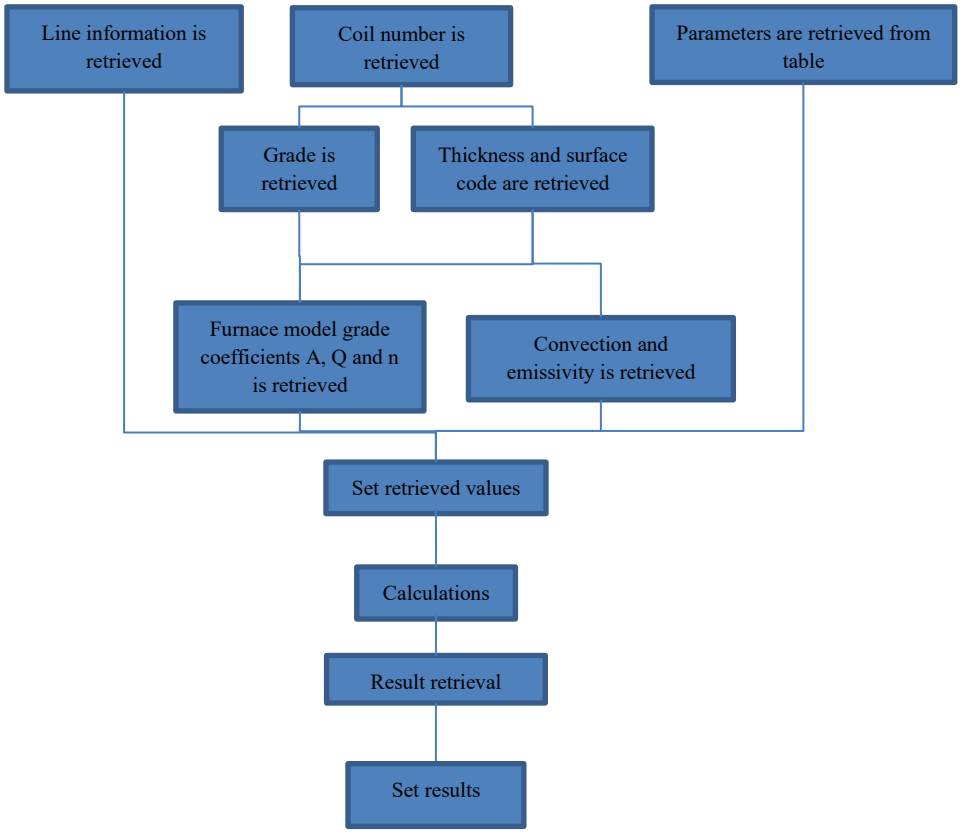


Figure 9. Set-point calculations flowchart.

Calculation of setpoints is an iterative process. The basic steps of calculation are as follow:

1. Start
2. Give zone 1 initial temperature
3. Increase other zone temperatures according to the temperature profile.
4. Check if zone temperature 2 is lower than *maxATMTemp*.
5. Check that coil temperature exiting zone is lower than zone temperature. If not, lower the temperature by *guessCoilInOutDiff*.
6. Use the grain size model to calculate resulting grain size.
7. If resulting grain size is the same as grain size target, move to step 10.
8. If resulting grain size < grain size target, increase the temperature of zone 1 step by *initZoneTempDiff* and move to step 3.
9. If resulting grain size > grain size target, decrease the temperature of zone 1 step by *initZoneTempDiff* and move to step 3.
10. End

## 5.3 Validating grain growth and furnace model

### 5.3.1 Grain growth calculation

The first task of the project was to check that all the input values, such as dimensions, work phase, temperatures and speed are passed and focused to the right coil in furnace model and grain size calculations. As previously mentioned, these input values are either from RETU or they are process data.

Manninen (2020a) concludes in his final report concerning AP-line furnace model development that the heat transfer and grain size calculations are correct. When phase two started, it was discovered that the previously mentioned values are not passed on correctly. This led to long period of testing and bug fixing. This phase wasn't officially finished by then, but in his report he finds it unlikely that new errors will be found in the future. He confirmed this later in private discussion. Double-checking the values is still required and within the scope of this project, as well as double-checking that models are calculating right, despite phase 1 declared complete.

Excel tool made by Manninen was translated from source code to Visual Basic -language to reach results in line with the ones calculated by automation. Like the automation, this Excel tool takes line speed, zone temperatures and other values as inputs and outputs grain size and strip temperatures at the end of each zone. Originally calculation of coil temperature was separate module from grain size calculation, but for this project the modules were combined for ease of use.

Initially comparisons were made using line speeds, furnace temperatures and strip temperatures received from MELA_ARCH-database. Automation calculated mean grain sized were added to comparison. Database included multiple results from different parts of the process, and they were averaged for each coil. Automation calculated grain size was compared to results received from Excel -calculation tables developed previously for furnace validation project. These Excel tools were validated in previous project and were deemed reliable. Some inaccuracy was to be expected, since excel tool used interpolation to determine strip in the zone based on inputted zone exit temperatures of the coil. Determining coil temperature every second using interpolation is significantly denser in terms of calculation points.

When code running the model itself calculates grain size, zone is divided into ten parts. It starts with the result of previous zone, and adds one tenth of the difference between the starting temperature and exit temperature at a time to accurately calculate the temperature.

Calculations were done from both the beginning using furnace temperatures to calculate strip temperatures and readily available measured strip temperatures from database. Measured grain sizes from quality control were added to comparison when available, but they can be somewhat unreliable when calculations are done using coils nominal thickness due to the fact that samples taken were only from one end, no scrapping is generally done before sample if the sample comes from AP3 and the method to measure grain size differs from usually used, so they were included only for reference.

Values used in calculations were received from lines logging data. The log saves used process parameters every five seconds, providing sufficient data point frequency. Log files included calculated strip temperatures and grain size making comparisons simpler.

The initial calculations using Excel-tool quickly ran into issues. The strip temperatures received from automation and self-calculated ones differed quite a bit, and this resulted in grain size differences up to 1,5 units when translated into ASTM grain size. The grain size calculated by line automation landed generally somewhere in the middle of these two self-calculated values.

The initial observations from strip temperatures were that strip temperatures received from database always had temperature at the end of zone 1 at 600 °C, while self-calculated values had no such requirements. Secondly, calculated strip temperatures were consistently higher than values provided by database. Thirdly, validity of used parameters such as emissivity and convection coefficient couldn't be determined, since they weren't displayed in variable interface of AP3-line automation. It was then concluded that logging the calculation was required for this phase.

The furnace atmosphere temperatures from log files were compared with signals received from PDA-files, which record signals and their values. As seen in appendix 2 figure 14, these values were identical when one hour of data was compared. The difference is that calculations only use the data every five seconds. The same can be seen when comparing line speeds. Figure 10 shows that when compared, line speeds seen in PDA and log files are identical.

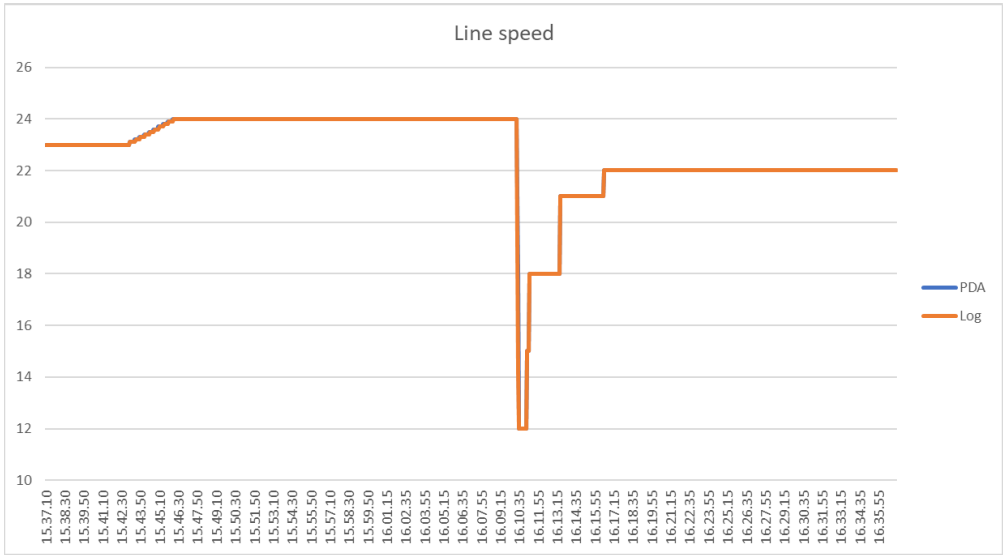


Figure 10. Line speed comparison.

From logging data it was determined the grain size calculation based on zone specific coil temperatures was working properly. It was noticed that the zone lengths used in calculations weren't the originally thought 15,5/15,5/11,5/11/9,15/6,15/10,15. Zone lengths of 11,25/11,25/8,73/8,73/8,73 were tried, and they gave somewhat accurate results. The comparison can be seen in table 7. Determining how these coil temperatures were calculated was more challenging. Logging data included values for strip emissivity, convection coefficients, line speed, furnace atmosphere temperature, physical dimensions and furnace zone lengths, but calculations using these values didn't match strip temperatures written in the logging files. The results can be seen in table 8. It was noted, that calculated stirp temperatures were lower than logged temperatures. The difference was especially pronounced during pre-heating.

| Time | Thickness | Width | Grade | Automation calculated grain size | Self calculated grain size |
|---|---|---|---|---|---|
| 18.46.45 | 2,99 | 1543 | 720-1 | 8,97 | 8,96 |
| 18.46.50 | 2,99 | 1543 | 720-1 | 8,948 | 8,94 |
| 18.50.00 | 3,00 | 1542 | 720-1 | 9,302 | 9,27 |
| 18.46.55 | 2,99 | 1543 | 720 | 8,949 | 8,94 |

Table 7. Grain size comparison

| Time | 20.4.2021 0:30:00 | |
|---|---|---|
| Zone number | Logged coil temperatures (°C) | Calculated zone temperature (°C) |
| Zone 1 | 143,6 | 88 |
| Zone 2 | 183,09 | 144 |
| Zone 3 | 566,34 | 484 |
| Zone 4 | 740,27 | 698 |
| Zone 5 | 968,11 | 914 |
| Zone 6 | 1070,73 | 1029 |
| Zone 7 | 1095,89 | 1071 |

Table 8. Coil temperature comparison.

It was discovered, that calculations for pre-heating zones began to roughly match when zone lengths of 31 m and 11,25 m were used. When compared to the real length of the furnace this is incorrect, since the pre-heat furnace itself is 31 m long. This meant that the zone temperatures matched with zone lengths were incorrect, and it was safe to assume that coil temperatures were incorrect too. While it was previously assumed that zone lengths of 15,5/15,5/11,25/11,25/8,73/8,73/8,73 were used in grain size calculations, it was determined that full zone lengths for the seven zones used in calculations were incorrectly 31/11,25/11,25/8,73/8,73/8,73/8,73. The grain size model factors in time spent in temperatures where grain growth is possible, so the zone length issue wasn't noticed previously. This was due to PARAMETERS table including parameters for both GRAINSIZE and SETPOINT. Zone lengths differed between these two parameter sets.

The logging data included multiple sets for grain size, emissivities, zone lengths and zone temperatures and these values were tested for strip temperature calculations. Using the source code of calculations, it was determined that instead of directly coming from FURNACETUNING -table like initially assumed, zone specific strip emissivities were temperature corrected using equation (36).

$$\varepsilon_z = \varepsilon_{z0} - e_c \times (T_\varepsilon - T_g) \tag{36}$$

where $\varepsilon_{z0}$ is emissivity of the strip in the zone as received from FURNACETUNING -table, $e_c$ is emissivity correction factor, $T_\varepsilon$ is the emissivity temperature level and $T_g$ is the absolute atmosphere temperature of the zone. The emissivities from FURNACETUNING -table are 0,45/0,45/0,59/0,59/0,643/0,643/0,643, used $T_\varepsilon$ was 1100 and used $e_c$ was 0,000118. As seen in table 9, using these temperature corrected emissivities with assumed zone lengths yielded results that aligned with zone specific coil temperatures from log files. The inaccuracies can be attributed to inaccuracies in numerical calculation.

| Zone Number | 1 | 2 | 3 | 4 | 5 | 6 | 7 |
|---|---|---|---|---|---|---|---|
| Time (s) | 49 | 67 | 84 | 98 | 112 | 126 | 140 |
| Calculated coil exit temperature (°C) | 179 | 230 | 594 | 748 | 935 | 1057 | 1081 |
| Coil exit temperature from log (°C) | 178,94 | 229,24 | 593,64 | 748,12 | 934,64 | 1057,12 | 1080,44 |

Table 9. Comparison between calculated and logged coil temperature from 20.4.2021 18.46.55

The zone lengths in GRAINSIZE group of parameters were changed to match the ones from SETPOINT group. These lengths were verified with log files, and relevant part of it can be seen in table 10. As can be seen from the table, new values were correctly applied.

| Date | Time | | Parameter | Value |
|---|---|---|---|---|
| 2021-05-20 | 02:30:00,050 | [15] | zoneLengths[0] | 15.5 |
| 2021-05-20 | 02:30:00,050 | [15] | zoneLengths[1] | 15.5 |
| 2021-05-20 | 02:30:00,050 | [15] | zoneLengths[2] | 11.5 |
| 2021-05-20 | 02:30:00,050 | [15] | zoneLengths[3] | 11 |
| 2021-05-20 | 02:30:00,050 | [15] | zoneLengths[4] | 9.15 |
| 2021-05-20 | 02:30:00,050 | [15] | zoneLengths[5] | 6.9 |
| 2021-05-20 | 02:30:00,050 | [15] | zoneLengths[6] | 10.15 |

Table 10. Used zone lengths from log files.

### 5.3.2 Set-point calculation

Set-point calculations were largely unvalidated before this project. Set-point calculations problems quickly became rather apparent. Based on the logging data, all variables that weren't associated with grain size calculations were constants. Source code was inspected. Calculation of grain size and set-points are divided into two different modules that are mostly similar. Differences appear in module that calls the values used in calculations and then the calculation modules.

The issue with Set-point calculation was that the constant values retrieved were saved in SPexchange -table. SPexchange -table isn't supposed to be used as a table from which values are retrieved, but as a table where values are saved for inspection. The flowchart has been visualized in figure 11.

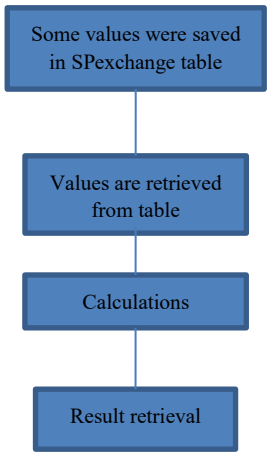


Figure 11. Set-point calculation flowchart

Fixing this issue with set-point calculations was discussed with ABB and fixing this issue had to be postponed. It was decided internal tool was necessary. The tool could be used to validate the current logic, determine parameters and calculate set-points for production experiments.

The tool was developed using source code of set-point calculations furnace model. Originally code was written in C#, but it was decided that tool would be written in C++. The first working version was finalized, and testing could be started. Initial testing and tweaking were done using online code complier. The first version was hardcoded meaning input values are put directly into the code. The meaningful inputs are process line speed, steel grade, thickness and width. The first version only included grain growth parameters for Polarit 720, and the parameters were also hard coded.

First issue that was noticed was that the set-point calculations use one many zones in their calculations. Unlike the grain size model, pre-heating was correctly divided into two parts but there was an extra 8,7 m long zone at the end. This meant that combined with cooling length model had nine different cooling zones. This naturally caused calculated temperatures to be lower than was meant since the time spent inside furnace was longer than intended.

Second issue was the way model estimated furnace temperatures for pre-heat furnace. The model used two different parameters, *TempRelationPreHeat11* and *TempRelationPreHeat12*, to calculate temperatures for first two zones based on calculated temperature of the first zone of furnace 1, marked as zone 2 in code. Below are the equations used to calculate temperatures. The calculation of pre-heat zone temperatures in equations (37) and (38)

$$T_{g1} = T_{g2} - m_{11} \times \frac{L_0}{2} \tag{37}$$

$$T_{g0} = T_{g1} - m_{12} \times (\frac{L_1}{2} + \frac{L_0}{2}) \tag{38}$$

where $T_{g1}$ and $T_{g0}$ are the estimated pre-heat zone temperatures, $T_{g2}$ is the calculated zone temperature of zone 1, $m_{11}$ and $m_{12}$ are *TempRelationPreHeat11* and *TempRelationPreHeat12*, $L_0$ and $L_1$ are the specific zone lengths.

Two distinct temperatures are calculated while in reality only one temperature is measured from furnace temperatures. This meant that for the sake of parity *atmTemps[0]* was set to equal *atmTemps[1]*. This was done by setting parameter

*TempRelationPreHeat12* to 0. Zone lengths are static, so pre-heating furnace temperature in calculation is just a static amount lower than first zone of furnace 1.

Issues were noticed in initial grain sizes in both grain size and set-point calculation furnace models. The model was supposed to retrieve either *initGrainsizeColdRolled* or *initGrainsizeHotRolled* based on *surfacecode*. Based on source code, parameter *initGrainsizeColdRolled* is statically retrieved so changes were required to this process to take *surfacecode* into account. Initial grain size is especially meaningful when calculated grain size is small. When resulting grain size is large, initial grain size is relatively meaningless when it comes to calculated grain size.

## 5.4 Parameter validation

Model-based furnace control and grain size calculation has been successfully in use in other AP lines. Largest documentation has been done for RAP5 line. Parameters for heat transfer, such as emissivity and convection coefficient, are to be scaled to AP3 using strip temperature measurements and tools like grain size calculation model and Excel tool.

Grain growth parameters were copied in a similar fashion from RAP5 line. This project included only austenitic grades, so only they were copied. Since the grain growth parameters are determined using laboratory experiments, the initial assumption was that they wouldn't need large modifications when copied from one line to another. As noted by Manninen (2020a), optimal grain growth parameters can be different for hot and cold rolled steels.

### 5.4.1 Disparity between grain size and set-point parameters

Disparity between parameters of grain size calculation and set-point calculations was an issue. The two models calculated resulting grain size in similar way, so it was natural that they should use the same parameters. The current and finalized parameters are seen in

appendix 3. The relevant differences are *emissivityCorrection* and *emissivityTempLevel* that control the emissivity changes based on temperature, *minTempCapacity* and *maxTempCapacity* that deal with temperature capacity of the strip and *GrainSzTolerance* which is used to determine acceptable grain size. There are other differences such as *iniSpeed* and *maxGrainsize*, but in reality they don't affect the results of calculations due to not being needed in the model.

As previously noted, grain size calculation gave relatively accurate results. For this reason the parameters from grain size calculations were mostly chosen to be copied to set-point calculations excluding some that were deducted to be better as the ones from SETPOINT group.

Changes to how pre-heating temperature was calculated during set-point calculations were explained in 5.3.2. *TempRelationPreHeat11* was left as the result determining parameter. Pre-heating furnace cannot be directly controlled by set-points, so the parameter must be determined based on history data. Aggregating saved furnace temperatures from 2000 datapoints and averaging difference between pre-heat and first zone of furnace 1 gave difference of 505 °C. This in turn translates to *TempRelationPreHeat11* value of 65,2.

Issue arises from the fact that in reality the temperature of the pre-heating furnace doesn't accurately correlate with temperature of furnace 1. The difference in the dataset between these two fluctuated between 382,2 °C and 599,4 °C. The lowest temperature of the pre-heat furnace in the dataset was 559,5 °C and average 630,8 °C. With lower line speeds set-point calculation gives lower temperatures and with *TempRelationPreHeat11* -value of 65,2 the estimated pre-heating temperature can be unrealistically low. Lower *TempRelationPreHeat11* result in higher calculated temperature. *TempRelationPreHeat11* -value of 60 gives the difference of 465 °C. Running the code with input values given in table 11. The grain growth parameters are the ones of Polarit 720. In table 12 are the resulting temperature targets for each zone. This example gives pre-heating temperature of 612,84 °C. Compared to the average pre-heating temperature from dataset, the difference is 17,96 °C. Pre-heating temperature doesn't have large

impact on resulting grain size due to how radiation as heat transfer mechanism related to temperature, so even 50 °C difference doesn't have a major impact on calculation results.

| Input | Value |
|---|---|
| Line speed | 30 m/min |
| Width | 1,271 m |
| Thickness | 0,0030044 m |
| A | 944507 |
| n | 0,29940 |
| Q | 133190 |

Table 11. Test inputs

| Zone temperature targets | Value (°C) |
|---|---|
| PreTemp1Target | 612,84 |
| PreTemp2Target | 612,84 |
| ZoneTemp1Target | 1077,84 |
| ZoneTemp2Target | 1082,84 |
| ZoneTemp3Target | 1087,84 |
| ZoneTemp4Target | 1092,84 |
| ZoneTemp5Target | 1097,84 |

Table 12. Calculated set-points.

### 5.4.2 Grain growth parameters

Grain growth parameters for this model are based on study conducted by Koskiniemi (1998). He determined parameters for Polarit grades 720-2, 725-2, 731-1, 750-1, 757-2 and 761-1. These parameters can be used for pretty much every Polarit grade sharing the main grade. The values can be seen in table 13. Corresponding values form AP3 automation are listed in table 14.

| Grade | A | Q | n |
|---|---|---|---|
| 720-2 | 659558 | 132467 | 0,3951 |
| 725-2 | 944507 | 133190 | 0,2994 |
| 731-1 | 444492786 | 205406 | 0,2501 |
| 750-1 | 2041986 | 147906 | 0,4089 |
| 757-2 | 3767364 | 155713 | 0,3231 |
| 761-1 | 69636280 | 188445 | 0,3366 |

Table 13. Grain growth parameters by Koskiniemi (1998)

| Grade | A | Q | n |
|---|---|---|---|
| 720-2 | 944507 | 133190 | 0,2994 |
| 725-2 | 944507 | 133190 | 0,2994 |
| 731-1 | 444492786 | 205406 | 0,2501 |
| 750-1 | 444492786 | 205406 | 0,2501 |
| 757-1 | 2041986 | 147897 | 0,4089 |
| 761-1 | 69636280 | 188445,04 | 0,3366 |

Table 14. Original AP3 grain growth parameters for the same grades.

As it can be seen, there are major differences between the two. It seems like the parameters were incorrectly copied from somewhere.

### 5.4.3 Statistical validation

Statistical analysis was used in addition to measurements to determine the accuracy of calculations. Data was collected from Polarit grades 720, 725, 731, 750 and 761 to determine if there were systematic issues with the model or the grade specific grain growth parameters. Measured grain size was collected using measurements from quality control samples and calculations were done using average zone temperatures and line speeds recorded in database. Database had limited amount of measurement points per coil, so if there were large changes during annealing it might reflect on average temperatures. Grain size measurements from 720 being the most common grade have the

largest sample size, followed by 750. 725 and titanium alloyed 731 and 761 have limited sample size.

The difference histograms can be seen in appendix 4 figures 15… 24. The difference is calculated using measured ASTM and subtracting calculated grain size from it, meaning positive value signifies that measured grain size was smaller than calculated one, and vice versa. The closer values are to 0, more accurate the calculations are. The grain growth parameters used were the original ones from table 14. Alternative results were calculated for some grades, and they are mentioned separately.

As can be seen from figure 15, using current parameters Polarit 720 shows that generally calculated grain size is too large with concentration peak being in 0,6… 0,9 bracket. Using parameters provided by Koskieniemi (1998) and initial grain size of 7 µm didn't improve the accuracy, but rather increased the calculated grain size (figure 16). It is somewhat expected that measured grain size to be larger than calculated, since many of these samples are taken from AP3 where the sample might be thicker than nominal thickness because the strip isn't scrapped from ends when the sample is taken ensuring the thickness is within tolerance. It seems that based on these results the original parameters are better for Polarit 720 than the ones provided by Koskiniemi. They are also used at RAP5 supporting this.

Polarit 725 original parameters matched with parameters by Koskiniemi (1998). The sample size is limited, but the accuracy of calculations is good (figure 17). No changes seem necessary.

Polarit 750 had large issues with parameters. This grade contains coils which have ASTM target of 10. The original parameters proved insufficient for calculating these coils, and the ASTM difference between calculated and measured was 2,5… 3 meaning according to calculations grain size would grow very little or wouldn't grow at all. The original model used parameters meant for 731 by Koskiniemi (1998). Using parameters meant for 750 by Koskiniemi and initial grain size of 7 µm the accuracy was extremely good as can be seen in figure 18. This figure includes Polarit 750-M which is mostly these tightly controlled grain size target ASTM 10 coils. 750-M was filtered away in figure 19 leaving

only 750-2, and the spread resembles 720 with original parameters in that the calculated grain size is too large. For comparison, 750-2 using original parameters and initial grain size is shown in figure 20. There the calculated grain size is too small. Considering the difference is expected to be positive due to thickness of samples, the parameters provided by Koskiniemi and initial grain size of 7 μm seem to be relatively accurate.

This leaves grades 731 and 761. 761 seems relatively accurate, since original parameters matched the ones by Koskiniemi (figure 21). 731 has very small sample size. Few samples are measured monthly, and not every coil had information on database. figure 22 shows that the calculated grain size is a lot smaller than measured grain size. RAP5 uses the same parameters for 731 hot strip as it uses for 725 hot strip. Those parameters were tested and the results are shown is figure 23. The results are better, but they can't really be used to decide which parameters to use. The parameters used at RAP5 for cold strip and parameters determined by Kurkela (2019) are even more aggressive when it comes to retarding grain growth, so in theory it wouldn't make much sense for hot rolled strip to use parameters that allow grain growth to happen so much easier.

Statistical analysis on grain size yielded mostly accurate results, but every grade had couple of coils which had significant differences between measured and calculated grain size. Couple of Polarit 720-1 coils are in table 15 as an example. The table shows coils, their thickness, grade, measured grain size, date of inspection, calculated grain size based on mean zone temperatures, grain size curve flatness if available and the difference between the two grain sizes. As it can be seen, grain size curve flatness is generally good meaning grain size calculations should be somewhat accurate assuming there were no issues with the sample. The issues could arise from process speeds changes for example, since the grain size was calculated using average speeds and temperatures. Process speed could change due to previous coils being thinner or thicker, or there were problems with the production line which required speeding up or slowing the line down.

| Slab | Thickness | Polarit-grasde | Measured grain size (ASTM) | Inspection day | Calculated grain size | Grain size curve flatness | Difference |
|---|---|---|---|---|---|---|---|
| 330062 | 4 | 720-1 | 7 | 20210621 | 8,32 | Good | -1,32 |
| 334126 | 8 | 720-1 | 8 | 20210704 | 6,7 | Good | 1,3 |
| 334121 | 8 | 720-1 | 8 | 20210704 | 6,7 | Good | 1,3 |
| 333441 | 8 | 720-1 | 6 | 20210705 | 7,75 | Good | -1,75 |
| 332726 | 8 | 720-1 | 7 | 20210710 | 8,26 | No data | -1,26 |
| 342402 | 2,99 | 720-1 | 10 | 20210729 | 8,24 | Bad | 1,76 |
| 344982 | 2,99 | 720-1 | 9,5 | 20210729 | 7,71 | Good | 1,79 |

Table 15. Inspected coils and their properties.

### 5.4.4 Initial grain size

As mentioned in 5.4.3, during statistical inspection a significant disparity was noticed between automation calculated grain size and excel tool calculated grain size when calculating grade 750-M which had ASTM target of 10. The initial grain size used in excel tool was 4 µm as it was the value given to *initGrainsizeHotRolled* in automation parameter tables. It turned out that automation was incorrectly using *initGrainsizeColdRolled,* which had initial value of 3 µm. This meant that if there was little to no increase in grain size in annealing, resulting grain size could have a difference of 1 ASTM when going from for example 13,2 ASTM to 12,2 ASMT.

*initGrainsizeHotRolled* value of 4 µm was placed under scrutiny. Tikkanen (2015) measured grain size from one hot rolled strip before annealing, and found that there was a difference based on measurement direction and the grain was flattened, as can be seen in figure 12. She measured mean grain size of 10,8 ASTM which translates to 7,6 µm. Grain size model form hot rolling plant supports this size. Data was retrieved for coils used in first production experiment, and the estimated grain size is between 6,5 µm and 10 µm. This combined with statistical analysis of Polarit 750 would suggest that 7 µm is a proper *initGrainsizeHotRolled* -value.

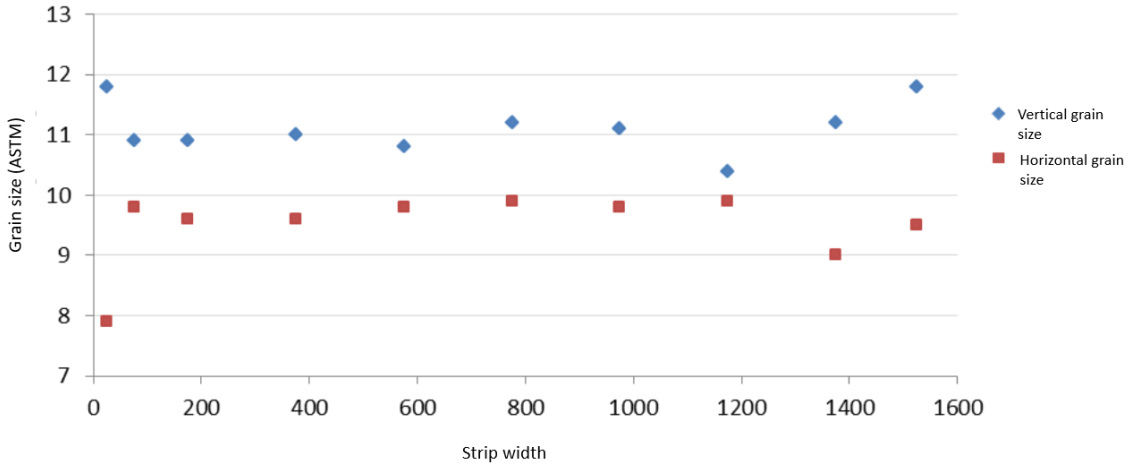


Figure 12. Grain size of black hot rolled strip vertically and horizontally. (Tikkanen 2015, modified)

# 6 PRODUCTION TRIALS

## 6.1 Fist production trial

### 6.1.1 Test method

Set-points were calculated in advance using previously mentioned external tool with the grain size target of 8,5 ASTM. Calculated set-points are shown in table 16 together with coils grade, width, thickness and target speed. Due to production schedule not yielding to the experiment, the experiment was done to the coils that happened to be in production without attention to the grade or thickness that were used. Initially the idea was to use couple of coils from Polarit grades 720, 725, 731, 750 and 761. Since most of the coils handled were Polarit 720-1 and other grades were singles and too thick, 720-1 ended up being the only grade with samples properly representing used set-points. Due to production technical demands coils 6,5 mm thick and thicker require extensions, and taking samples from such coils would have required extra work phases and thus those coils were skipped from experiment.

Grain size measurements were done according to ASTM E 112 -13. X Cross chord pattern was used, grain size was measured based on five different pictures taken at ¼ depth. Comparison calculations were done using Excel tool with realized zone temperatures and line speeds. There are still issues with saved grain size curve, so comparisons don’t include those. Relevant parties were informed of this issue.

The production experiment ran into some issues due to issues with production line. Welding machine malfunctioned and caused furnace stop. During furnace stop furnace temperatures are lowered, and driving them back up and accelerating speed to pre-stop levels takes time and causes grain size to go awry. There were other technical difficulties which caused the production line to stop in the afternoon. There were communication errors that caused coils from 344405-00 onward to be annealed using usual zone temperatures instead of calculated temperatures. The samples annealed using incorrect temperatures were deemed useful to tune parameters, so they are shown here.

| Coil | Thicknes s (mm) | Grade | Width (mm) | Linespeed (m/min) | Pre-heat estimate (°C) | Zone 1 (°C) | Zone 2 (°C) | Zone 3 (°C) | Zone 4 (°C) | Zone 5 (°C) |
|---|---|---|---|---|---|---|---|---|---|---|
| 342284 | 2,99 | 731-1 | 1286 | 40 | 682 | 1147 | 1152 | 1157 | 1162 | 1167 |
| 343421 | 2,99 | 750-2 | 1032 | 40 | 682 | 1147 | 1152 | 1157 | 1162 | 1167 |
| 344261 | 2,99 | 720-1 | 1037 | 40 | 658 | 1123 | 1128 | 1133 | 1138 | 1143 |
| 344262 | 2,99 | 720-1 | 1037 | 40 | 658 | 1123 | 1128 | 1133 | 1138 | 1143 |
| 344267 | 2,99 | 720-1 | 1035 | 40 | 658 | 1123 | 1128 | 1133 | 1138 | 1143 |
| 344301 | 2,99 | 720-1 | 1039 | 40 | 658 | 1123 | 1128 | 1133 | 1138 | 1143 |
| 318191 | 2,99 | 725-1 | 1040 | 40 | 658 | 1123 | 1128 | 1133 | 1138 | 1143 |
| 342281 | 3 | 731-1 | 1280 | 40 | 682 | 1147 | 1152 | 1157 | 1162 | 1167 |
| 344424 | 2,99 | 720-1 | 1546 | 40 | 658 | 1123 | 1128 | 1133 | 1138 | 1143 |
| 344441 | 2,99 | 720-1 | 1545 | 40 | 658 | 1123 | 1128 | 1133 | 1138 | 1143 |
| 344426 | 2,99 | 720-1 | 1545 | 40 | 658 | 1123 | 1128 | 1133 | 1138 | 1143 |
| 344425 | 2,99 | 720-1 | 1545 | 40 | 658 | 1123 | 1128 | 1133 | 1138 | 1143 |
| 344422 | 3 | 720-1 | 1546 | 40 | 658 | 1123 | 1128 | 1133 | 1138 | 1143 |
| 341306 | 3,49 | 725-1 | 1282 | 38,6 | 676 | 1141 | 1146 | 1151 | 1156 | 1161 |
| 344405 | 3,49 | 720-1 | 1548 | 34,3 | 655 | 1120 | 1125 | 1130 | 1135 | 1140 |
| 326872 | 4,49 | 724-1 | 1545 | 26,7 | 649 | 1114 | 1119 | 1124 | 1129 | 1134 |
| 326792 | 4,49 | 725-8 | 1544 | 26,7 | 649 | 1114 | 1119 | 1124 | 1129 | 1134 |
| 344565 | 5,99 | 720-1 | 1543 | 20 | 643 | 1107 | 1112 | 1117 | 1122 | 1127 |
| 326853 | 5,99 | 724-1 | 1545 | 20 | 643 | 1107 | 1112 | 1117 | 1122 | 1127 |

Table 16. Calculated zone temperature set-points.

### 6.1.2 Results

Realized zone temperatures at the beginning and end of each coil can be seen in tables 17 and 18 respectively. During production experiment it was noticed that zone 2 didn't follow temperature set-points. When using set-point at stabilized temperature, zone 2 had trouble surpassing 1050 °C. This is mostly noticeable with coils 344424-00, 344426-00 and 344422-00 where temperature should have been 1128 °C. A person knowledgeable on these matters was interviewed to figure out possible explanations. According to him,

the lines sensors and blowers have had issues. Furnace might also have leaks that affect one specific zones. Finding and fixing those issues fall outside this project.

| Coil | Thickness (mm) | Grade | Width (mm) | Line speed (m/min) | Pre-heat (°C) | Zone 1 (°C) | Zone 2 (°C) | Zone 3 (°C) | Zone 4 (°C) | Zone 5 (°C) |
|---|---|---|---|---|---|---|---|---|---|---|
| 318191 | 2,99 | 725-1 | 1040 | 28 | 723 | 1126 | 1110 | 1130 | 1125 | 1133 |
| 342281 | 3 | 731-1 | 1280 | 40 | 704 | 1086 | 1100 | 1112 | 1126 | 1130 |
| 344424 | 2,99 | 720-1 | 1546 | 40 | 705 | 1050 | 1054 | 1084 | 1161 | 1179 |
| 344426 | 2,99 | 720-1 | 1545 | 40 | 593 | 1132 | 1044 | 1129 | 1138 | 1144 |
| 344422 | 3 | 720-1 | 1546 | 40 | 555 | 1127 | 1026 | 1129 | 1138 | 1144 |
| 341306 | 3,49 | 725-1 | 1282 | 7 | 703 | 1208 | 1154 | 1244 | 1239 | 1144 |
| 344405 | 3,49 | 720-1 | 1548 | 34 | 739 | 1182 | 1159 | 1186 | 1169 | 1143 |
| 326872 | 4,49 | 724-1 | 1545 | 27 | 580 | 1174 | 1046 | 1193 | 1159 | 1059 |
| 326792 | 4,49 | 725-8 | 1544 | 26 | 556 | 1182 | 1060 | 1179 | 1215 | 1095 |
| 344565 | 5,99 | 720-1 | 1543 | 20 | 538 | 1189 | 1051 | 1178 | 1204 | 1097 |
| 326853 | 5,99 | 724-1 | 1545 | 20 | 514 | 1186 | 1042 | 1165 | 1206 | 1088 |

Table 17. Realized line speeds and zone temperatures at the beginning of each coil.

| Coil | Thickness (mm) | Grade | Width (mm) | Line speed (m/min) | Pre-heat (°C) | Zone 1 (°C) | Zone 2 (°C) | Zone 3 (°C) | Zone 4 (°C) | Zone 5 (°C) |
|---|---|---|---|---|---|---|---|---|---|---|
| 318191 | 2,99 | 725-1 | 1040 | 32 | 779 | 1155 | 1165 | 1220 | 1229 | 1241 |
| 342281 | 3 | 731-1 | 1280 | 40 | 756 | 1147 | 1154 | 1157 | 1161 | 1183 |
| 344424 | 2,99 | 720-1 | 1546 | 40 | 581 | 1123 | 1040 | 1140 | 1136 | 1139 |
| 344426 | 2,99 | 720-1 | 1545 | 40 | 556 | 1125 | 1035 | 1133 | 1138 | 1146 |
| 344422 | 3 | 720-1 | 1546 | 40 | 533 | 1120 | 1028 | 1132 | 1138 | 1143 |
| 341306 | 3,49 | 725-1 | 1282 | 16 | 687 | 1134 | 1136 | 1150 | 1159 | 1160 |
| 344405 | 3,49 | 720-1 | 1548 | 34 | 573 | 1166 | 1079 | 1178 | 1138 | 1052 |
| 326872 | 4,49 | 724-1 | 1545 | 25 | 545 | 1193 | 1056 | 1178 | 1211 | 1092 |
| 326792 | 4,49 | 725-8 | 1544 | 26 | 540 | 1184 | 1051 | 1172 | 1210 | 1097 |
| 344565 | 5,99 | 720-1 | 1543 | 20 | 538 | 1187 | 1042 | 1165 | 1204 | 1090 |
| 326853 | 5,99 | 724-1 | 1545 | 17,5 (14) | 556 | 1176 | 1039 | 1164 | 1208 | 1088 |

Table 18. Realized line speeds and zone temperatures at the end of each coil.

Grain sizes were measured from each sample. 344565-00 had only one sample taken. Measured grain size and sample thicknesses are given in table 19. Based on the

measurements sample thicknesses were significantly larger than nominal thicknesses especially with 3 mm thick coils. As expected, coils 318191-00… 344422-00 have too small grain size.

| Coil | Nominal thickness (mm) | Grade | Sample thickness 01 (mm) | Sample thickness 02 (mm) | Measured grain size 01 (ASTM) | Measured grain size 02 (ASTM) |
|---|---|---|---|---|---|---|
| 318191 | 2,99 | 725-1 | 3,77 | 3,16 | 8,3 | 8,8 |
| 342281 | 3 | 731-1 | 3,75 | 3,51 | 10 | 11,2 |
| 344424 | 2,99 | 720-1 | 3,86 | 3,33 | 10,2 | 9,4 |
| 344426 | 2,99 | 720-1 | 4 | 3,4 | 10,1 | 9,8 |
| 344422 | 3 | 720-1 | 3,93 | 3,38 | 10,1 | 8,7 |
| 341306 | 3,49 | 725-1 | 3,77 | 3,78 | 8,8 | 6,8 |
| 344405 | 3,49 | 720-1 | 3,69 | 3,78 | 6,9 | 8,6 |
| 326872 | 4,49 | 724-1 | 4,69 | 4,55 | 7,3 | 6,8 |
| 326792 | 4,49 | 725-8 | 4,66 | 4,64 | 6,9 | 6,1 |
| 344565 | 5,99 | 720-1 | - | 6,29 | - | 8,2 |
| 326853 | 5,99 | 724-1 | 6,16 | 6,15 | 7 | 5,1 |

Table 19. Sample thicknesses and measured grain sizes.

Calculated grain sizes are shown in table 20. Calculations were done for both nominal thickness and actual sample thickness. Line speed for coil 341306-00 was too low to make meaningful calculations.

| Coil | Calculated grain size based on nominal thickness 01 (ASTM) | Calculated grain size based on nominal thickness 02 (ASTM) | Calculated grain size based on sample thickness 01 (ASTM) | Calculated grain size based on sample thickness 02 (ASTM) |
|---|---|---|---|---|
| 318191 | 7,13 | 5,91 | 7,81 | 5,23 |
| 342281 | 10,52 | 8,02 | 12,7 | 9,19 |
| 344424 | 8,74 | 9,12 | 10,85 | 9,87 |
| 344426 | 9,03 | 9,13 | 11,46 | 10,06 |
| 344422 | 9,21 | 9,26 | 11,54 | 10,17 |
| 341306 | - | - | - | - |
| 344405 | 7,2 | 8,93 | 7,57 | 9,46 |
| 326872 | 8,61 | 7,43 | 8,9 | 7,75 |
| 326792 | 7,64 | 7,8 | 7,89 | 7,97 |
| 344565 | 7,71 | 7,92 | - | 8,24 |
| 326853 | 7,96 | 7,08 | 8,13 | 6,17 |

Table 20. Calculated grain sizes based on nominal thickness and sample thickness.

Coil measured coil temperatures were retrieved from database. They can be seen in tables 21 and 22. They are used to calculate competing grain size results and for comparing calculated coil temperatures. Zone 1 measurement isn't functioning, and it shows constant 600 °C, but it isn't really relevant since temperature is too low in this zone to cause grain growth.

| Coil | Thickness (mm) | Grade | Width (mm) | Line speed (m/min) | Zone 1 (°C) | Zone 2 (°C) | Zone 3 (°C) | Zone 4 (°C) | Zone 5 (°C) |
|---|---|---|---|---|---|---|---|---|---|
| 318191 | 2,99 | 725-1 | 1040 | 28 | 600 | 1057 | 1049 | 1100 | 1110 |
| 342281 | 3 | 731-1 | 1280 | 40 | 600 | 886 | 922 | 993 | 1043 |
| 344424 | 2,99 | 720-1 | 1546 | 40 | 600 | 819 | 859 | 1061 | 1110 |
| 344426 | 2,99 | 720-1 | 1545 | 40 | 600 | 841 | 916 | 1020 | 1080 |
| 344422 | 3 | 720-1 | 1546 | 40 | 600 | 829 | 902 | 1010 | 1074 |
| 341306 | 3,49 | 725-1 | 1282 | 7 | 600 | 1250 | 1218 | 1239 | 1082 |
| 344405 | 3,49 | 720-1 | 1548 | 34 | 600 | 1172 | 1114 | 1130 | 1096 |
| 326872 | 4,49 | 724-1 | 1545 | 27 | 600 | 865 | 930 | 1126 | 1119 |
| 326792 | 4,49 | 725-8 | 1544 | 26 | 600 | 903 | 978 | 1098 | 1129 |
| 344565 | 5,99 | 720-1 | 1543 | 20 | 600 | 884 | 959 | 1103 | 1134 |
| 326853 | 5,99 | 724-1 | 1545 | 20 | 600 | 883 | 950 | 1069 | 1110 |

Table 21. Measured coil temperatures at the beginning of each coil.

| Coil | Thickness (mm) | Grade | Width (mm) | Line speed (m/min) | Zone 1 (°C) | Zone 2 (°C) | Zone 3 (°C) | Zone 4 (°C) | Zone 5 (°C) |
|---|---|---|---|---|---|---|---|---|---|
| 318191 | 2,99 | 725-1 | 1040 | 28 | 600 | 1123 | 1161 | 1208 | 1215 |
| 342281 | 3 | 731-1 | 1280 | 40 | 600 | 1243 | 1097 | 1142 | 1164 |
| 344424 | 2,99 | 720-1 | 1546 | 40 | 600 | 856 | 920 | 1023 | 1077 |
| 344426 | 2,99 | 720-1 | 1545 | 40 | 600 | 840 | 909 | 1017 | 1075 |
| 344422 | 3 | 720-1 | 1546 | 40 | 600 | 839 | 907 | 1017 | 1076 |
| 341306 | 3,49 | 725-1 | 1282 | 7 | 600 | 1158 | 1088 | 1133 | 1153 |
| 344405 | 3,49 | 720-1 | 1548 | 34 | 600 | 1010 | 961 | 1056 | 1067 |
| 326872 | 4,49 | 724-1 | 1545 | 27 | 600 | 923 | 995 | 1091 | 1123 |
| 326792 | 4,49 | 725-8 | 1544 | 26 | 600 | 900 | 975 | 1081 | 1118 |
| 344565 | 5,99 | 720-1 | 1543 | 20 | 600 | 887 | 959 | 1065 | 1107 |
| 326853 | 5,99 | 724-1 | 1545 | 20 | 600 | 881 | 958 | 1065 | 1107 |

Table 22. Measured coil temperatures at the end of each coil.

### 6.1.3 Verification of results

Calculated coil temperatures were compared with measured coil temperatures with specific coils. Comparisons are shown in table 23. Measured coil temperatures are saved as whole numbers, while calculated results are given with one decimal. It can be seen that

zone 2 has large difference between calculated and measured temperature. This can be somewhat explained by pyrometer emissivity in this specific zone. As can be seen in table 24, zone 2 has pyrometer emissivity of 0,9. As explained in 3.1.2., accurate pyrometer temperature requires surface emissivity to be known. Since the temperature of the strip at zone 2 is low, emissivity might not reach this value of 0,9 while zone 4 and 5 having higher strip temperature have more accurate result. As explained in 4.3, the lowest pyrometer calibration temperature is 900 °C, so accuracy below that is questionable. Based on these results heat transfer model doesn't require large changes at least for thin coils.

| Coil calculated/measured | Zone 1 (°C) | Zone 2 (°C) | Zone 3 (°C) | Zone 4 (°C) | Zone 5 (°C) |
|---|---|---|---|---|---|
| 344424 01 calculated | 527,8 | 744,9 | 895,3 | 1007,3 | 1109,3 |
| 344424 01 measured | 600 | 819 | 859 | 1061 | 1110 |
| 344426 01 calculated | 549,0 | 752,5 | 930,1 | 1016,8 | 1090,0 |
| 344426 01 measured | 600 | 841 | 916 | 1020 | 1080 |
| 344422 01 calculated | 527,3 | 724,4 | 912,7 | 1005,9 | 1085,1 |
| 344422 01 measured | 600 | 829 | 902 | 1010 | 1074 |
| 344424 02 calculated | 533,1 | 738,4 | 929,2 | 1015,3 | 1086,1 |
| 344424 02 measured | 600 | 856 | 920 | 1023 | 1077 |
| 344426 02 calculated | 525,6 | 729,5 | 918,7 | 1009,7 | 1088,1 |
| 344426 02 measured | 600 | 840 | 909 | 1017 | 1075 |
| 344422 02 calculated | 511,8 | 714,6 | 908,8 | 1003,3 | 1083,3 |
| 344422 02 measured | 600 | 839 | 907 | 1017 | 1076 |

Table 23. Coil temperature comparisons at the beginning (01) and end (02) of each coil.

| Zone | 1 | 2 | 3 | 4 | 5 |
|---|---|---|---|---|---|
| Emissivity | 0,9 | 0,9 | 0,95 | 0,95 | 0,95 |

Table 24. Pyrometer emissivity.

Comparisons between different calculations and measured grain size are shown in tables 25, 26 and 27. Generally grain size calculated based on nominal thickness is too large, and grain size calculated based on actual sample thickness is too small. Some calculations

were done using parameters by Koskiniemi and initial grain size of 7 µm and mixes of those two. These calculations used sample thickness unless specified otherwise. Statistical validation showed that original parameters were better for Polarit 720 than the ones by Koskiniemi. Polarit 750 showed that accuracy improved around ASTM 10 range when initial grain size increased. The initial grain size seemed to be especially important when it came to accuracy of under annealed coils. Based on these results, most accurate results for grade 720 are when initial grain size is 7 µm and parameters by Koskiniemi are used. This contradicts the results from statistical validation. The final conclusion is that which parameters 720 uses isn't really relevant, as long as initial grain size of 7 µm is used.

| Coil | Measured grain size | Calculated grain size using nominal | Grain size with actual thickness (ASTM) | 720 alternative |
|---|---|---|---|---|
| 318191 | 8,3 | 7,13 | 7,81 | |
| 342281 | 10 | 10,52 | 12,7 | |
| 344424 | 10,2 | 8,74 | 10,85 | 10,86 |
| 344426 | 10,1 | 9,03 | 11,46 | 11,41 |
| 344422 | 10,1 | 9,21 | 11,54 | 11,49 |
| 341306 | 8,8 | | | |
| 344405 | 6,9 | 7,2 | 7,57 | 7,31 |
| 326872 | 7,3 | 8,61 | 8,9 | 8,72 |
| 326792 | 6,9 | 7,64 | 7,89 | |
| 344565 | | 7,71 | | |
| 326853 | 7 | 7,96 | 8,13 | 7,91 |

Table 25. Coil beginning grain size comparisons.

| Coil | Measured grain size | Calculated grain size using nominal thickness | Grain size with actual thickness (ASTM) | 720 alternative |
|---|---|---|---|---|
| 318191 | 8,8 | 5,91 | 5,23 | |
| 342281 | 11,2 | 8,02 | 9,19 | |
| 344424 | 9,4 | 9,12 | 9,87 | 9,85 |
| 344426 | 9,8 | 9,13 | 10,06 | 10,05 |
| 344422 | 8,7 | 9,26 | 10,17 | 10,17 |
| 341306 | 6,8 | | | |
| 344405 | 8,6 | 8,93 | 9,46 | 9,32 |
| 326872 | 6,8 | 7,43 | 7,75 | 7,31 |
| 326792 | 6,1 | 7,8 | 7,97 | |
| 344565 | 8,2 | 7,92 | 8,24 | 8,02 |
| 326853 | 5,1 | 7,08 | 6,17 | 5,86 |

Table 26. Coil end grain size comparisons.

| Coil | Measured grain size | 720 alternative parameters | initial grain size 7 µm and alternative parameters | initial grain size 7 µm and original parameters |
|---|---|---|---|---|
| 344424.01 | 10,2 | 10,86 | 10,21 | 10,36 |
| 344426.01 | 10,1 | 11,41 | 10,5 | 10,65 |
| 344422.01 | 10,1 | 11,49 | 10,53 | 10,68 |
| 344405.01 | 6,9 | 7,31 | 7,27 | 7,43 |
| 344424.02 | 9,4 | 9,85 | 9,54 | 9,68 |
| 344426.02 | 9,8 | 10,05 | 9,69 | 9,83 |
| 344422.02 | 8,7 | 10,17 | 9,77 | 9,91 |
| 344405.02 | 8,6 | 9,32 | 9,11 | 9,33 |

Table 27. Polarit 720 comparisons.

The first production trial was done before statistical analysis was complete, so the observations from those weren't used in this production trial. They were implemented to the second production trial instead. Most notably initial grain size of 7 µm would have given more accurate set-points.

## 6.2 Second production trial

### 6.2.1 Test method

Similar to first production experiment, zone temperature set-points were calculated in advance based on grade, thickness, width and nominal line speed. The focus was on Polarit 750 since this grade had the largest changes made and lacked samples from previous test. The coils, their physical dimensions, line speeds and calculated zone temperature set-points are shown in table 28.

Changes made to the calculations from the first production experiment were limiting zone 2 temperature to 1050 °C, changing the initial grain size to 7 µm and changing grain growth parameters of Polarit 750 to match the ones suggested by Koskiniemi (1998).

| Coil | Thickness (mm) | Grade | Width (mm) | Line speed (m/min) | Pre-heat estimate (°C) | Zone 1 (°C) | Zone 2 (°C) | Zone 3 (°C) | Zone 4 (°C) | Zone 5 (°C) |
|---|---|---|---|---|---|---|---|---|---|---|
| 354824 | 5,99 | 761-1 | 1286 | 20 | 688 | 1153 | 1050 | 1163 | 1168 | 1173 |
| 355482 | 5,99 | 750-2 | 1032 | 20 | 661 | 1126 | 1050 | 1136 | 1141 | 1146 |
| 355481 | 6 | 750-2 | 1037 | 20 | 661 | 1126 | 1050 | 1136 | 1141 | 1146 |
| 31633G | 5,99 | 720-2 | 1037 | 20 | 655 | 1120 | 1050 | 1130 | 1135 | 1140 |
| 31615H | 5,99 | 720-2 | 1035 | 20 | 655 | 1120 | 1050 | 1130 | 1135 | 1140 |
| 30599H | 4,49 | 750-2 | 1039 | 30 | 697 | 1162 | 1050 | 1172 | 1177 | 1182 |
| 30599K | 4,5 | 750-2 | 1040 | 30 | 697 | 1162 | 1050 | 1172 | 1177 | 1182 |

Table 28. Calculated zone temperature set-points**.**

During discussion with line operators, they mentioned that zone 5 temperature of 1182 °C might be too high. High temperature causes flames to come out of the furnace, which is unfavorable to say the least. This caused new values to be calculated using lower line speeds for 354824-00, 30599H-00 and 30599K-00. These new zone temperature set-points and line speeds are shown in table 29.

| Coil | Thickness (mm) | Grade | Width (mm) | Line speed (m/min | Pre-heat estimate (°C) | Zone 1 (°C) | Zone 2 (°C) | Zone 3 (°C) | Zone 4 (°C) | Zone 5 (°C) |
|---|---|---|---|---|---|---|---|---|---|---|
| 354824 | 5,99 | 761-1 | 1286 | 17 | 658 | 1123 | 1050 | 1133 | 1138 | 1143 |
| 355482 | 5,99 | 750-2 | 1032 | 20 | 661 | 1126 | 1050 | 1136 | 1141 | 1146 |
| 355481 | 6 | 750-2 | 1037 | 20 | 661 | 1126 | 1050 | 1136 | 1141 | 1146 |
| 31633G | 5,99 | 720-2 | 1037 | 20 | 655 | 1120 | 1050 | 1130 | 1135 | 1140 |
| 31615H | 5,99 | 720-2 | 1035 | 20 | 655 | 1120 | 1050 | 1130 | 1135 | 1140 |
| 30599H | 4,49 | 750-2 | 1039 | 25 | 658 | 1123 | 1050 | 1133 | 1138 | 1143 |
| 30599K | 4,5 | 750-2 | 1040 | 25 | 658 | 1123 | 1050 | 1133 | 1138 | 1143 |

Table 29. New calculated zone temperature set-points.

Grain size measuring method and comparison calculation methods are the same as in the first production trial.

### 6.2.2 Results

Measured zone temperatures for beginning and end of each coils are shown in tables 30 and 31 respectively. Tables also include realized line speeds.

| Coil | Thickness (mm) | Grade | Width (mm) | Line speed (m/min) | Pre-heat (°C) | Zone 1 (°C) | Zone 2 (°C) | Zone 3 (°C) | Zone 4 (°C) | Zone 5 (°C) |
|---|---|---|---|---|---|---|---|---|---|---|
| 354824 | 5,99 | 761-1 | 1286 | 17 | 475 | 1125 | 1031 | 1189 | 1213 | 1096 |
| 355482 | 5,99 | 750-2 | 1032 | 20 | 539 | 1117 | 1045 | 1133 | 1134 | 1143 |
| 355481 | 6 | 750-2 | 1037 | 20 | 475 | 1120 | 1010 | 1139 | 1143 | 1148 |
| 31633G | 5,99 | 720-2 | 1037 | 20 | 512 | 1113 | 1029 | 1119 | 1129 | 1127 |
| 31615H | 5,99 | 720-2 | 1035 | 20 | 499 | 1115 | 1010 | 1129 | 1136 | 1138 |
| 30599H | 4,49 | 750-2 | 1039 | 25 | 656 | 1110 | 1039 | 1128 | 1129 | 1132 |
| 30599K | 4,5 | 750-2 | 1040 | 25 | 620 | 1134 | 1055 | 1133 | 1140 | 1147 |

Table 30. Measured zone temperatures at the beginning of each coil.

| Coil | Thickness (mm) | Grade | Width (mm) | Line speed (m/min) | Pre-heat (°C) | Zone 1 (°C) | Zone 2 (°C) | Zone 3 (°C) | Zone 4 (°C) | Zone 5 (°C) |
|---|---|---|---|---|---|---|---|---|---|---|
| **354824** | 5,99 | 761-1 | 1286 | 17 | 540 | 1127 | 1045 | 1129 | 1132 | 1147 |
| **355482** | 5,99 | 750-2 | 1032 | 20 | 471 | 1128 | 1012 | 1137 | 1141 | 1157 |
| **355481** | 6 | 750-2 | 1037 | 20 | 477 | 1126 | 1012 | 1132 | 1141 | 1147 |
| **31633G** | 5,99 | 720-2 | 1037 | 20 | 487 | 1125 | 1010 | 1131 | 1137 | 1145 |
| **31615H** | 5,99 | 720-2 | 1035 | 20 | 492 | 1125 | 1008 | 1132 | 1136 | 1141 |
| **30599H** | 4,49 | 750-2 | 1039 | 25 | 630 | 1126 | 1056 | 1129 | 1137 | 1148 |
| **30599K** | 4,5 | 750-2 | 1040 | 25 | 600 | 1152 | 1041 | 1124 | 1133 | 1143 |

Table 31. Measured zone temperatures at the end of each coil.

The sample information from this production trial is shown in table 32. The table shows measured sample thickness and measured grain size.

| Coil | Nominal thickness (mm) | Grade | Sample thickness 01 (mm) | Sample thickness 02 (mm) | Measured grain size 01 (ASTM) | Measured grain size 02 (ASTM) |
|---|---|---|---|---|---|---|
| 354824 | 5,99 | 761-1 | 6,21 | 6,28 | 8,7 | 8,9 |
| 355482 | 5,99 | 750-2 | 6,16 | 6,38 | 8,7 | 9,5 |
| 355481 | 6 | 750-2 | 6,22 | 6,39 | 9,5 | 9,8 |
| 31633G | 5,99 | 720-2 | 6,06 | 6,16 | 8,7 | 8,4 |
| 31615H | 5,99 | 720-2 | 6,1 | 6,2 | 8,9 | 8,9 |
| 30599H | 4,49 | 750-2 | 4,69 | 4,86 | 8,8 | 8,9 |
| 30599K | 4,5 | 750-2 | 4,68 | 5,01 | 8,9 | 9,5 |

Table 32. Sample thicknesses and measured grain sizes.

### 6.2.3 Verification of results

Comparisons between calculated grain size using nominal thickness, actual sample thickness and measured grain size are shown in tables 33 and 34 for samples 1 (coil beginning) and 2 (coil end) respectively. Grain size using nominal thickness should be within 0,15 ASMT of 8,5. As it can be seen, calculated grain size is generally too small. This shows that zone temperatures didn't reach the zone temperature set-points used. One reason is insufficient control of zone 2, which was constrained to 1050 °C due to results of previous production trial. Second reason could be that pre-heat temperature wasn't

accurately estimated. The pre-heat temperatures were between 471 °C and 656 °C despite other zones not having drastic temperature shifts.

In an ideal scenario, the difference between measured grain size and grain size calculated using actual thickness would be very small. It can be seen from results that the calculation accuracy of Polarit 750 which was the focus of this trial is rather good largest error being 0,45 ASMT. Sample 1 of 354824-00 didn't stable zone temperatures and the temperatures were fluctuating at that point, so the accuracy is questionable. The differences were plotted into histogram for figure 13. Most results fall within expected margin of error 354824-00 beginning sample being the only real outlier.

| Coil | Grade | Nominal thickness (mm) | Actual thickness (mm) | Grain size with nominal thickness (ASTM) | Grain size with actual thickness (ASTM) | Measured grain size (ASTM) |
|---|---|---|---|---|---|---|
| 354824 | 761-1 | 5,99 | 6,21 | 7,94 | 8,19 | 8,7 |
| 355482 | 750-2 | 5,99 | 6,16 | 7,88 | 9,15 | 8,7 |
| 355481 | 750-2 | 6 | 6,22 | 9,05 | 9,29 | 9,5 |
| 31633G | 720-2 | 5,99 | 6,06 | 9,1 | 9,16 | 8,7 |
| 31615H | 720-2 | 5,99 | 6,1 | 8,95 | 9,06 | 8,9 |
| 30599H | 750-2 | 4,49 | 4,69 | 8,8 | 9,03 | 8,8 |
| 30599K | 750-2 | 4,5 | 4,68 | 8,43 | 8,66 | 8,9 |

Table 33. Sample 1 grain size comparison.

| Coil | Grade | Nominal thickness (mm) | Actual sample thickness (mm) | Grain size with nominal thickness (ASTM) | Grain size with actual thickness (ASTM) | Measured grain size (ASTM) |
|---|---|---|---|---|---|---|
| 354824 | 761-1 | 5,99 | 6,28 | 8,8 | 9,06 | 8,9 |
| 355482 | 750-2 | 5,99 | 6,38 | 8,94 | 9,36 | 9,5 |
| 355481 | 750-2 | 6 | 6,39 | 9,08 | 9,5 | 9,8 |
| 31633G | 720-2 | 5,99 | 6,16 | 8,81 | 8,99 | 8,4 |
| 31615H | 720-2 | 5,99 | 6,2 | 8,86 | 9,08 | 8,9 |
| 30599H | 750-2 | 4,49 | 4,86 | 8,49 | 8,93 | 8,9 |
| 30599K | 750-2 | 4,5 | 5,01 | 8,61 | 9,24 | 9,5 |

Table 34. Sample 2 grain size comparison.

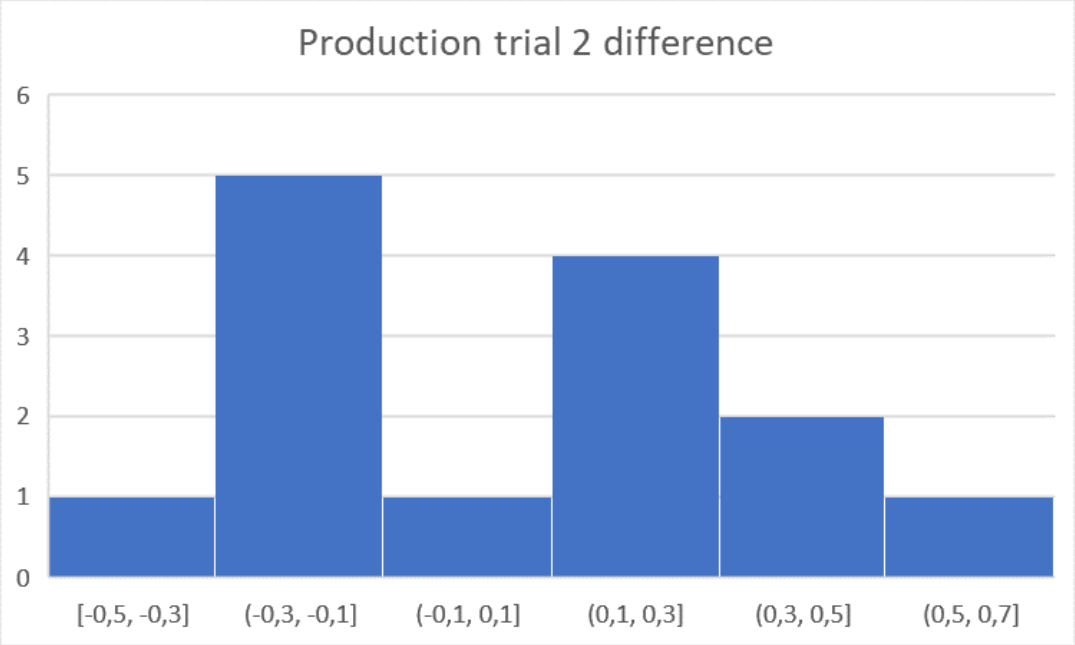


Figure 13. Difference between calculated and measured grain size.

Due to the high temperatures of zone 5 the temperature set-points had to be recalculated using lower line speeds. This could be changed using different temperature profile. Profile used in this and previous trial is rising profile, meaning every zone is hotter than the previous. Another option is limiting zone 5 temperature to 1140 °C. The achievable temperature of the zone is largely based on the used fuel. For example, zone 1 might not reach the same temperatures as zone 3 due to different fuel used. In table 35 is an example of typical profile of AP3 temperature profile, when the temperatures are controlled manually by operators. Zones 1 and 2 are rather static in their temperature, high temperature at zone 3 is used, and then then temperature becomes lower and lower. Something resembling this might be optimal. Currently *maxATMTemp* is around 1203 °C, and zone 3 regularly rises above that value during normal operations. This means that increase in this value is needed, if inverted temperature profile is used.

| Zone | 1 | 2 | 3 | 4 | 5 |
|---|---|---|---|---|---|
| Temperature (°C) | 1142 | 1057 | 1199 | 1148 | 1116 |

Table 35. Example profile.

Better option might be to program in separate zone maximum temperatures for each zone, so that changing the values is easy if extra work is put into improving furnace control. In the current tool 1050 °C is hard coded. Current limiters could be as the ones in table 36. If method like this is implemented, temperature profile wouldn't matter much.

| Zone | 1 | 2 | 3 | 4 | 5 |
|---|---|---|---|---|---|
| Temperature (°C) | 1150 | 1050 | 1210 | 1200 | 1145 |

Table 36. Tentative maximum zone temperatures.

# 7 CONCLUSIONS AND SUGGESTIONS FOR IMPROVEMENT

The project didn't reach all of its initial goals, but lot of information was discovered and improvements made. Dynamic set-point calculation isn't ready yet, but the background study was done to help and facilitate implementation work.

Updating automation to calculate set-points and use them during process is incomplete. Implementing these changes to automation wasn't done during the project, but ABB was requested to make the changes. Furnace control is still insufficient if extreme accuracy is needed from the automation especially when it comes to zone 2. According to latest information zone 2 accuracy development is under process in another project. Parameters were homogenized for grain size calculation and set-point calculation. They are shown in appendix 3. They were not yet implemented to automation tables as of writing these conclusions.

Grain size calculation was validated, requirements of modifications has been released. FurnaceModel -class requires that *initGrainSizeHotRolled* can be retrieved based on *surfacecode*. Zone lengths were changed to parameter tables in automation according to appendix 3. Usefulness of grain size calculation remains uncertain as long as grain size curves aren't properly saved into database. Relevant parties were informed of this problem

Set-point calculation was validated. External tool based on source code of the model was developed and it was determined to have sufficient accuracy in terms of the resulting grain size. Number of zones needs to be reduced to match real world amount. FurnaceModel -class requires that *initGrainSizeHotRolled* can be retrieved based on *surfacecode.* Setting furnace temperatures maximum for each zone would be good change, since changing the maximum temperatures would be easy and wouldn't require changing source code if furnace control is improved. Tentative limits were in table 36. If these limits were to be implemented, temperature profile wouldn't matter much.

After statistical analysis and measurements from production trial *initGrainSizeHotRolled* -parameter was changed from 4 to 7. Changes were made to Polarit 750 grain growth parameters. Changes not yet implemented to automation tables.

Annealing of cold rolled strips was left unvalidated. *Workphasecode* and grain size target relationship needs to be redefined in FurnaceModel -class.

# 8 SUMMARY

This thesis consists of theory part, where heat transfer mechanisms, grain growth and recrystallization phenomena are explained as well as annealing of austenitic stainless steel. Annealing furnace and its measurement and control are discussed. Some examples of how process parameters have been acquired have been provided.

Validation of the grain size and set-point calculation models was done through inspecting source code, available logging files and measured data. Production trials were done to help define process parameters and validate the operation of the production line using said calculation parameters.

Getting the understanding to effectively work with an automation system of complex process such as continuous annealing and pickling line is a large undertaking. Acquiring t Lacking documentation and unfinished, poorly written source code were major slowing factors in this work and the code could use some cleaning. Nevertheless, validation process was done for the grain size calculation and set-point calculation for austenitic grades, but all the changes weren't implemented yet.

Unfortunately, this project did not reach all the goals set to it in the beginning, but a lot of work was done to advance towards properly working automation. Annealing of cold rolled strips was left unvalidated, but some problems regarding it were discussed within this thesis. Hopefully this thesis can work as a documentation for the future work to be done and overall improved the knowledge of the studied processes.

# 9 REFERENCES

ABB, 2014. System 800xA System Guide Functional Description. Available: [https://library.e.abb.com/public/d9ce45e2f627f75dc1257dbd0043816c/3BSE038018-600_-_en_System_800xA_6.0_System_Guide_Functional_Description.pdf] Retrieved 23.8.2021

Connor, N., 2019. What is Logarithmic Mean Temperature Difference – LMTD – Definition. Thermal Engineering. Available: [https://www.thermal-engineering.org/what-is-logarithmic-mean-temperature-difference-lmtd-definition/]. Referenced 19.3.2021.

Cobo, S. J., Palmiere, E. J. and Rainforth, W. M., 2008. Mechanism of Oxidation of Austenitic Stainless Steels unde Conditions of Hot Rolling in Steckel Mills. Metallurgical and Materials Transactions A, 39A.

Gardner, L., Ng, K. T., 2006. Temperature development in structural stainless steel sections exposed to fire. Fire Safety Journal, 41.

Ginzbur, V. B., 2005. Metallurgical design of flat rolled steels. Marcel Dekker, Inc., U.S.A. ISBN 0-8247-5847-1.

Hewitt, G. F., Hires, G. L. and Bott, T. R., Process heat transfer. CRC Press, Inc., U.S.A. ISBN 0-8493-9918-1

Humphreys, F. J. and Hatherly, M., 1995. Recrystallization and related annealing phenomena. Pergamon, Oxford. First edition. ISBN 0-08-041884-8

Jaiswal, S., Farrugia, D., Huasin, Z., Ingham, P., Wilkinson, J. and Morris, P., 1996. Modelling of microstructure in rod rolling of alloy and stainless steels. European Commission, Luxembourg. ISBN 92-827-6899-6

Kivivuori, S. and Härkönen, S., 2004. Lämpökäsittelyoppi. Teknologiateollisuus ry, Helsinki. 2. edition. ISBN 951-817-849-6.

Koskiniemi, J., 1998. Polarit-terästen rakeenkasvun kinetiikka ja mallintaminen (HEKE-projekti). Outokumpu intranet, unpublished.

Kurkela, M., 2019. Modeling grain growth. Outokumpu intranet, unpublished.

Liu, Y. F., Hu, Z. L., Shi, D. H. and Yu, K., 2013. Experimental Investigation of Emissivity of Steel. International Journal of Thermophysics, 34, 7.

Liu, T., Long, M., He, W., Chen, D., Dong, Z., Zhang, X. and Duan, H., 2019. Prediction model for austenite grains growth during reheating process in Ti micro-alloyed cast steel by coupling precipitates dissolution and coarsening behavior. Journal of Iron and Steel Research International 26.

Manninen, T., 2020a. Final Report for the AP-line furnace model development -project. Outokumpu intranet, unpublished.

Manninen, T., 2020b. RAP5 -linjan uunimallin kuvaus. Technical report.

Microsoft, 2021. A tour of the C# language. Web document. Available [https://docs.microsoft.com/en-us/dotnet/csharp/tour-of-csharp/]

Outokumpu Oyj, 2015. V HP3 005 06. HP3-LINJAN TEKNISET RAJOITUKSET RULLILLE. Outokumpu Intranet, unpublished.

Outokumpu Oyj, 2017. Handbook of Stainless Steel. Outokumpu Oyj, Helsinki.

Outokumpu Oyj, 2021. Hehkutus- ja peittauslinjat oppisopimusluento, Outokumpu Intranet, unpublished.

Padilha, A., Dutra, J. and Randle, V., 1999. Interaction between precipitation, normal grain growth, and secondary recrystallisation in austenitic stainless steel containing particles. Materials Science and technology, 15 (6), p. 1009-1014.

Prieto, M., Fernández, F. and Rendueles, J., 2005. Thermal performance of annealing line heating furnace, Ironmaking & Steelmaking, 32, 2, 171-176

Rohsenow, W. M., Hartnett, J. P. and Cho, Y. I. Handbook of heat transfer. McGraw-Hill Companies, Inc., U.S.A. ISNB 0-07-053555-8

Shirdel, M., Mirzadeh, H. and Parsa, M., 2014. Abnormal grain growth in AISI 304L stainless steel. Materials Characterization 97, p. 11-17.

Su, F., 2017. Heating and Flow Analysis in Hot-Rolled Stainless Strip Continuous Annealing Furnace Based on CFD Modeling. Heat tRansfer-Asian Research, 46 (7), p. 924-932.

Švantner, M., Vacíková, P. and Honner, M., 2013. Non-contact charge temperature measurement on industrial continuous furnaces and steel charge emissivity analysis. Infrared Physics & Technology, 61

Tafreshi, O., Hoa., Shadmehri., F Hoang, D. and Rosca, D., 2020. Determination of convective heat transfer coefficient for automated fiber placement (AFP) for thermoplastic composites using hot gas torch. Advanced Manufacturing: Polymer & Composites Science, 6 (2), p. 86-100.

Uusitalo, J. Outokumpu HP3 L2 Kommuinkointi.

Webster, E., Saunders, P., 2020. Characterizing Drift Behavior in Type S Thermocouples to Predict In-use Temperature Errors. International Journal of Thermophysics 41, 5.

Woods, S., Jung, T., Sears, D. and Yu, J., 2014. Emissivity of silver and stainless steel from 80 K to 300 K: Application to ITER thermal shields. Cryogenics 60, p. 44-48.

Yoshitani, N., 1993. Modelling and Parameter Estimation for Strip Temperature Control in Continuous Annealing Processes. IECON Proceedings (Industrial Electronics Conference), 1, p. 469-474.

Zareba, S., Wolff, A. and Jelali, M., 2016. Mathematical modelling and parameter identification of a stainless steel annealing furnace. Simulation Modelling Practice and Theory 60, p. 15-39.

Appendix 1. Relevant parameter explanations (1)

| Variable | Explanation |
|---|---|
| TemperatureChangeForDerivate | Used for calculating energy balance |
| initGrainsizeColdRolled | Initial grain size for cold rolled coil |
| initGrainsizeHotRolled | Initial grain size for hot rolled coil |
| maxLineSpeed | Maximum allowed line speed |
| normalGrainsize | Grain size normal. |
| grainSzTolerance | Grain size tolerance |
| initTempZone3 | Initial zone 1 temperature for set-point calculation |
| speedStep | Lower speed if maximum allowed temperature is exceeded |
| maxATMTemp | Maximum allowed zone temperature |
| minAvgTemp | Used to determine which temperature capacities are used |
| initZoneTempDiff | Zone temperature adjustment if grain size |
| maxTempCapacity | Used with high coil temperatures |
| minTempCapacity | Used with low coil temperatures |
| tempCapacityCoeff1 | Temperature adjustment for maxTempCapacity |
| tempCapacityCoeff2 | Temperature adjustment for minTempCapacity |
| initCoilTemp | Coil temperature when arriving to furnace zone |
| goalEnergyBalDiff | Used to determine if energy equation is in balance |
| guessCoilInOutDiff | Used as coil temperature tolerance in comparisons |
| maxIters | Maximum number of iterations |

Table 37. Relevant parameter explanations.

Appendix 1. Relevant parameter explanations (2)

| Variable | **Explanation** |
|---|---|
| zoneLengths[0] | Length of preheat section divided by 2 |
| zoneLengths[1] | Length of preheat section divided by 2 |
| zoneLengths[2] | Length of furnace zone 1 |
| zoneLengths[3] | Length of furnace zone 2 |
| zoneLengths[4] | Length of furnace zone 3 |
| zoneLengths[5] | Length of furnace zone 4 |
| zoneLengths[6] | Length of furnace zone 5 |
| emissivityCorrection | Parameter for adjusting zone emissivity |
| emissivityTempLevel | Parameter for adjusting zone emissivity |
| usepyrotemps | Used to determine if pyrometer temperatures are used in calculation |

Table 38. Relevant parameter explanations continued.

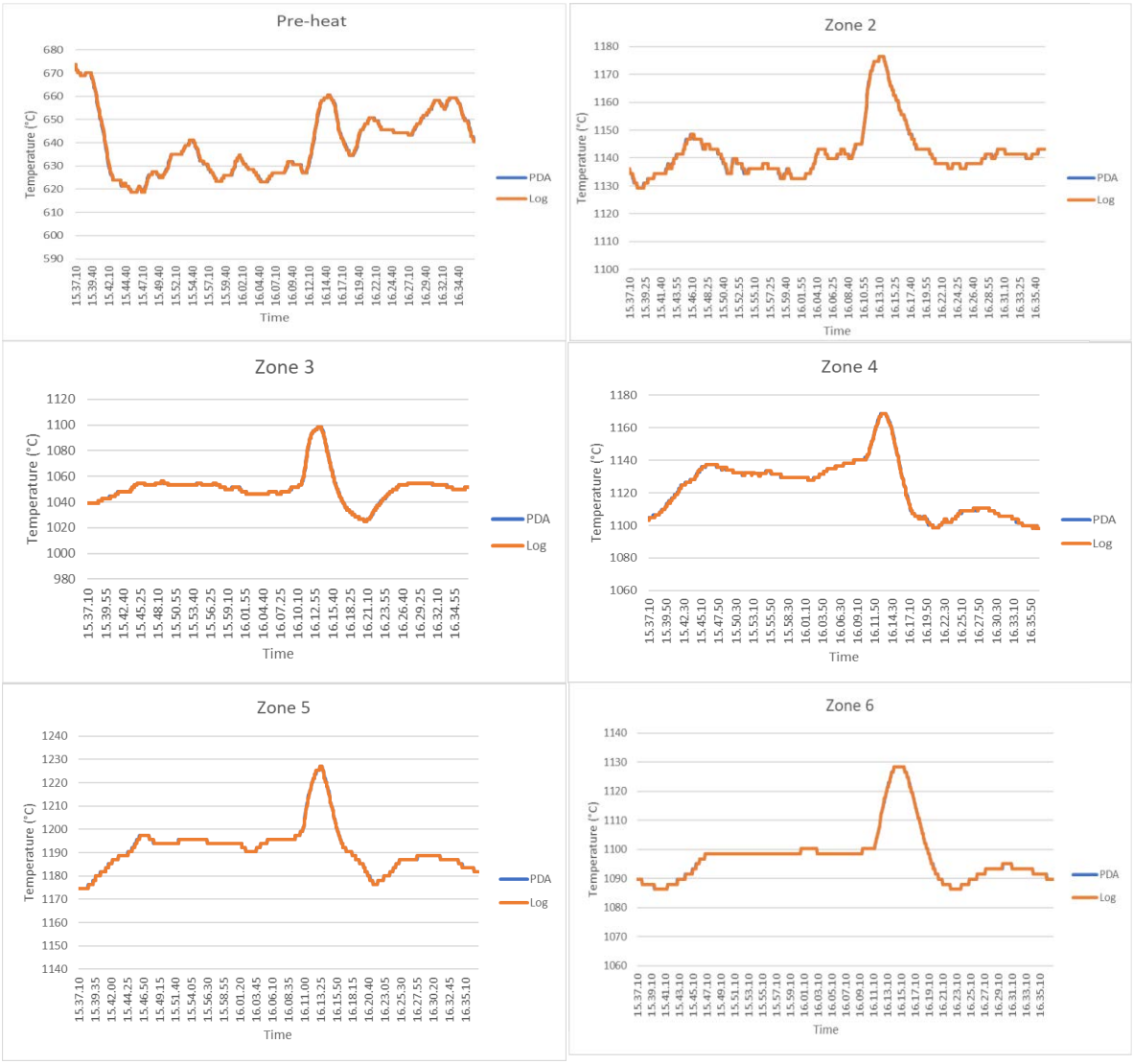


Figure 14. Temperature comparison between PDA-signals and log.

| Parameter name | SETPOINTS | GRAINSIZE | Final value |
|---|---|---|---|
| alphaCoeff | 0 | - | |
| CoolingLength | 5 | 5 | 5 |
| CoolingRate | 20 | 20 | 20 |
| emissivityCorrection | 0,000108 | 0,000118 | 0,000118 |
| emissivityTempLevel | 1423 | 1100 | 1100 |
| ferriticStripTempCorrection | 0 | | |
| goalEnergyBalDiff | 2000 | 2000 | 2000 |
| GrainSzTolerance | 0,15 | 0,3 | 0,15 |
| guessCoilInOutDiff | 3 | 3 | 3 |
| initCoilTemp | 298 | 298 | 298 |
| initGrainsizeColdRolled | 3 | 3 | 3 |

Table 39. Initial parameter values and final parameter values.

| Parameter name | SETPOINTS | GRAINSIZE | Final value |
|---|---|---|---|
| initGrainsizeHotRolled | 4 | 4 | 7 |
| initSpeed | 0,03 | 0,01 | 0,03 |
| initTempZone3 | 1273 | 1273 | 1273 |
| initZoneTempDiff | 3 | 3 | 3 |
| maxATMTemp | 1480 | 1523 | 1480 |
| maxGrainsize | 13 | 14 | 13 |
| maxIters1 | 200 | 200 | |
| maxIters2 | 300 | | |
| maxLineSpeed | 40 | 80 | 40 |
| maxTempCapacity | 462 | 422 | 422 |
| minAvgTemp | 400 | 400 | |
| minGrainsize | 3 | 3 | |
| minTempCapacity | 225 | 185,5 | 185,5 |

Table 40. Initial parameter values and final parameter values continued.

| Parameter name | SETPOINTS | GRAINSIZE | Final value |
|---|---|---|---|
| nominalSpeedFactor | 100 | | |
| normalGrainsize | 8 | 8,5 | 8,5 |
| speedStep | 0,55 | 0,55 | 0,55 |
| tempCapacityCoeff1 | 0,775 | 0,775 | 0,775 |
| tempCapacityCoeff2 | 0,148 | 0,148 | 0,148 |
| temperatureCorrection | 0 | | |
| TempRelationPreHeat11 | 8,5 | | 65 |
| TempRelationPreHeat12 | 7,5 | | 0 |
| zoneLenghts[0] | 15,5 | 15,5 | 15,5 |
| zoneLenghts[1] | 15,5 | 15,5 | 15,5 |
| zoneLenghts[2] | 11,5 | 11,5 | 11,5 |
| zoneLenghts[3] | 11 | 11 | 11 |
| zoneLenghts[4] | 9,15 | 9,15 | 9,15 |
| zoneLenghts[5] | 6,9 | 6,9 | 6,9 |
| zoneLenghts[6] | 10,15 | 10,15 | 10,15 |
| tempStep | | 20 | |
| tempStepEstimCoeff | | 100000 | |
| tempStepEstimOffset | | 0,1 | |
| usepyrotemps | | 0 | |
| minTempStep | | 0,01 | |

Table 41. Initial parameter values and final parameter values continued.

Appendix 4. Grain size difference histograms. (1)

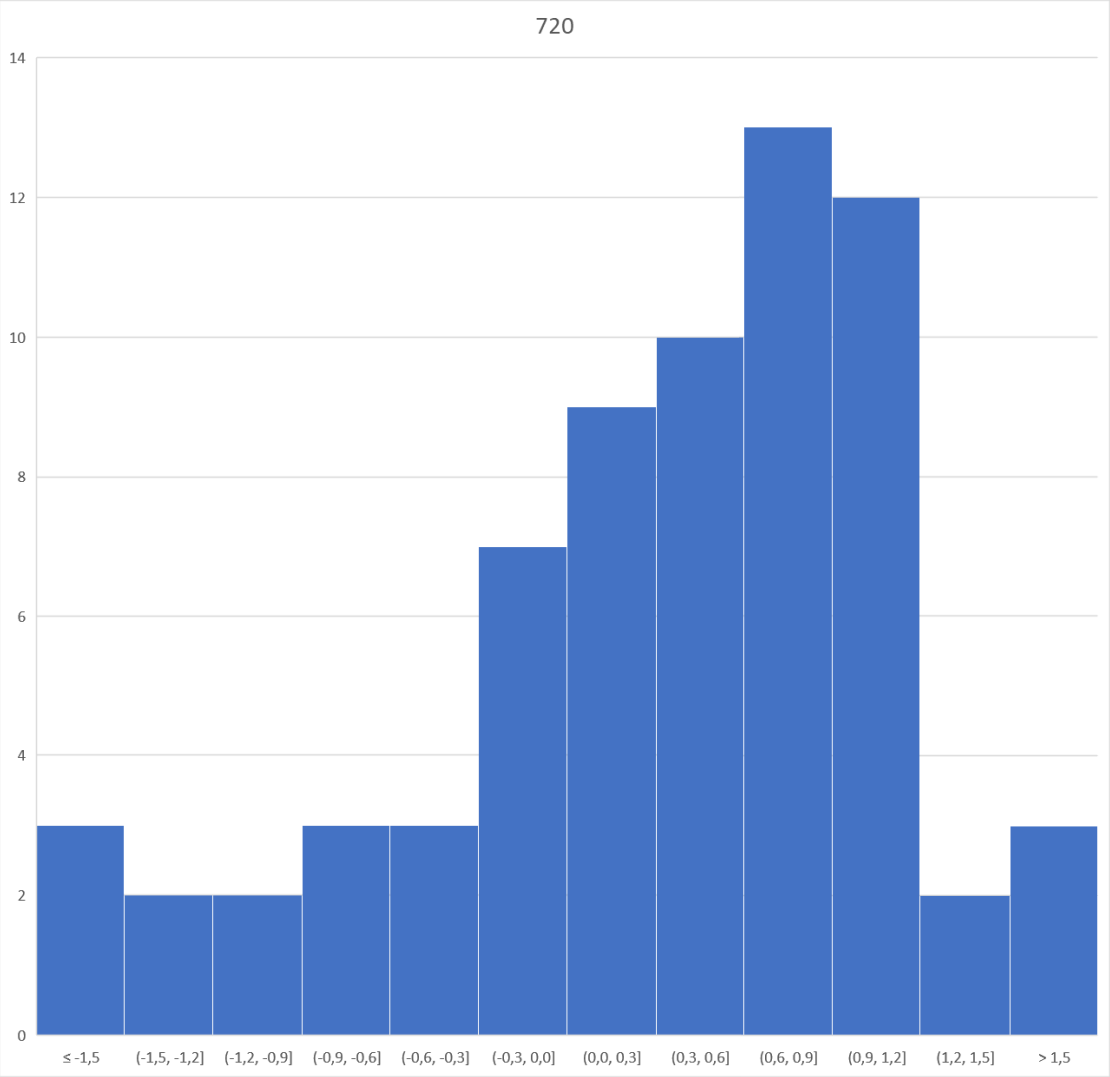


Figure 15. Histogram of difference between calculated and measured grain size of Polarit 720

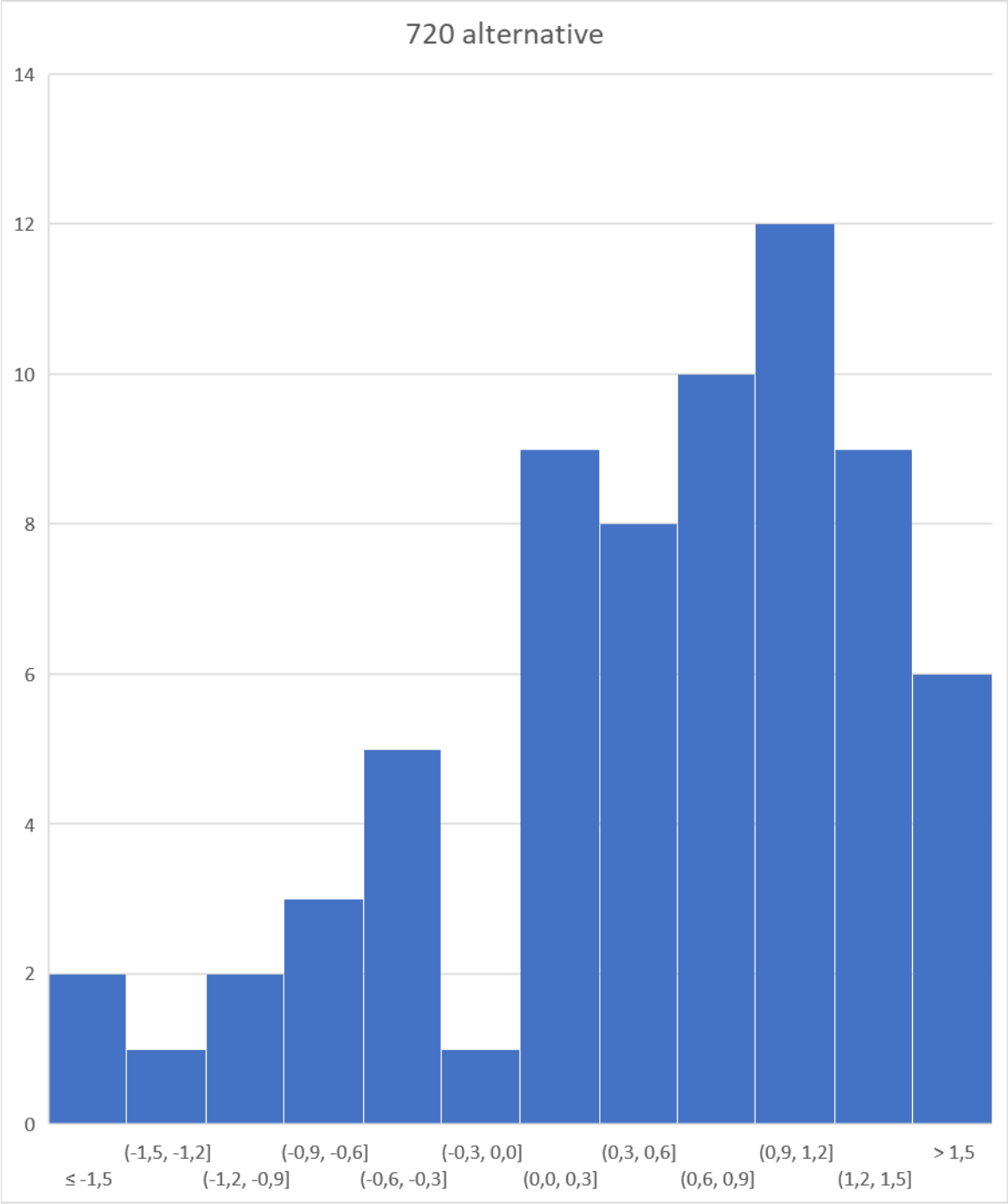


Figure 16. Histogram of difference between calculated and measured grain size of Polarit 720 using alternative parameters.

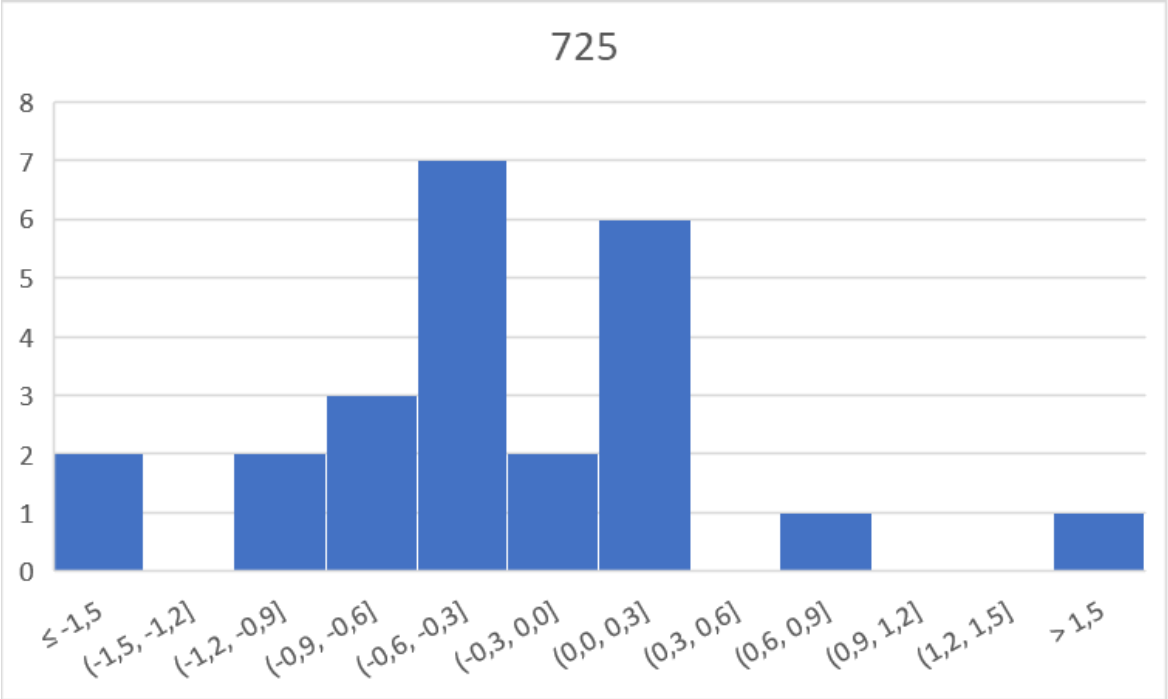


Figure 17. Histogram of difference between calculated and measured grain size of Polarit 725.

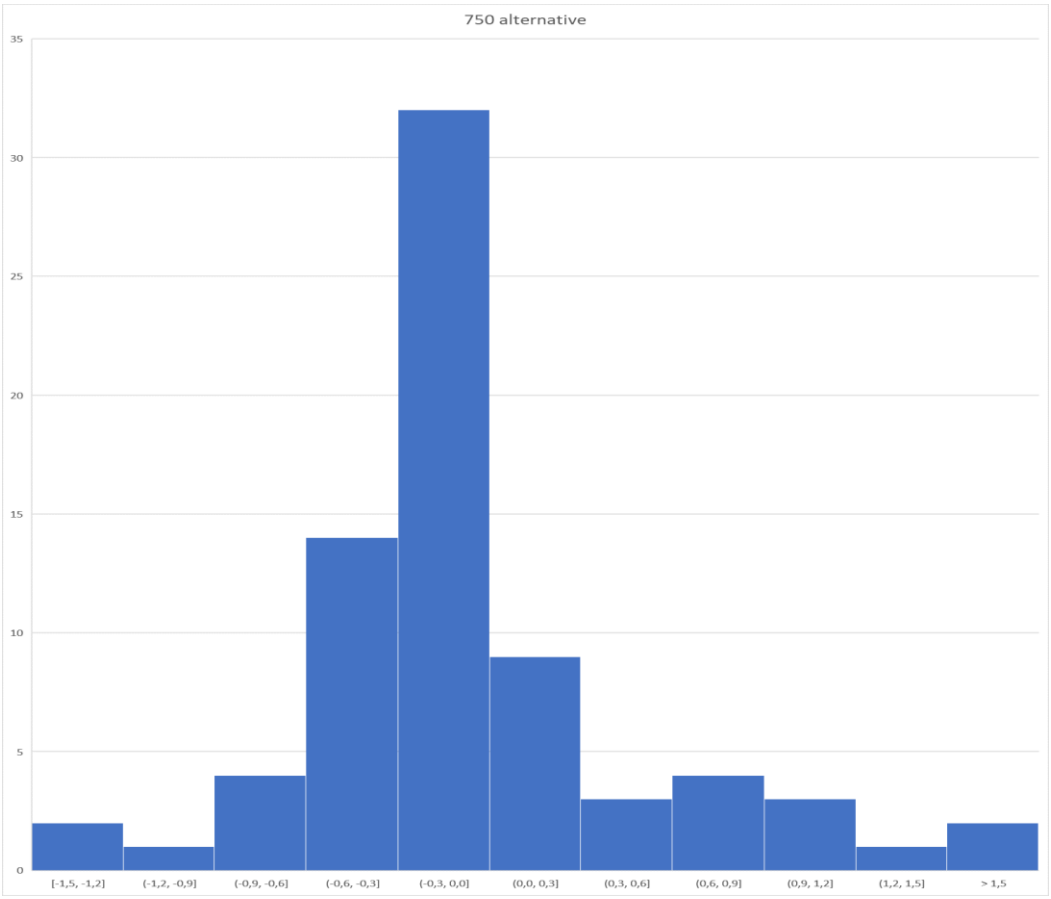


Figure 18. Histogram of difference between calculated and measured grain size of Polarit 750 using alternative parameters.

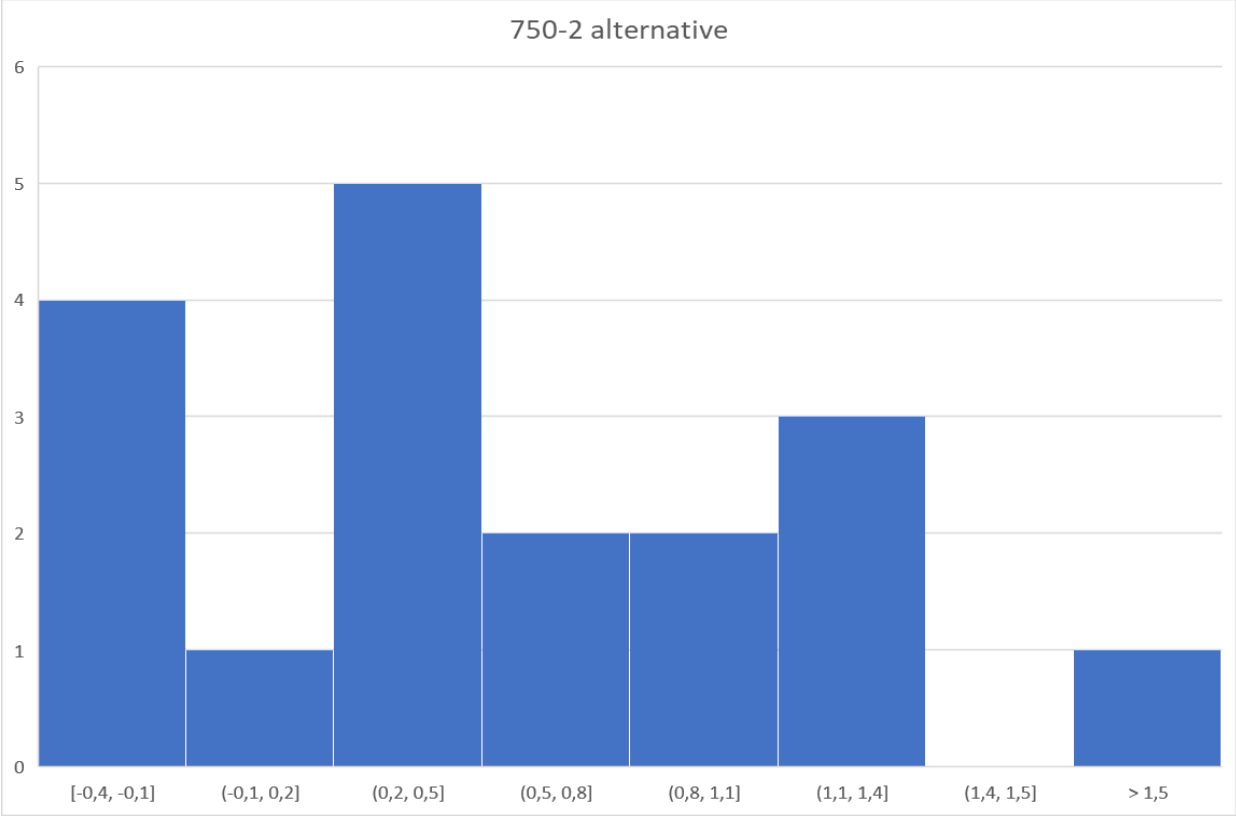


Figure 19. Histogram of difference between calculated and measured grain size of Polarit 750-2 using alternative parameters.

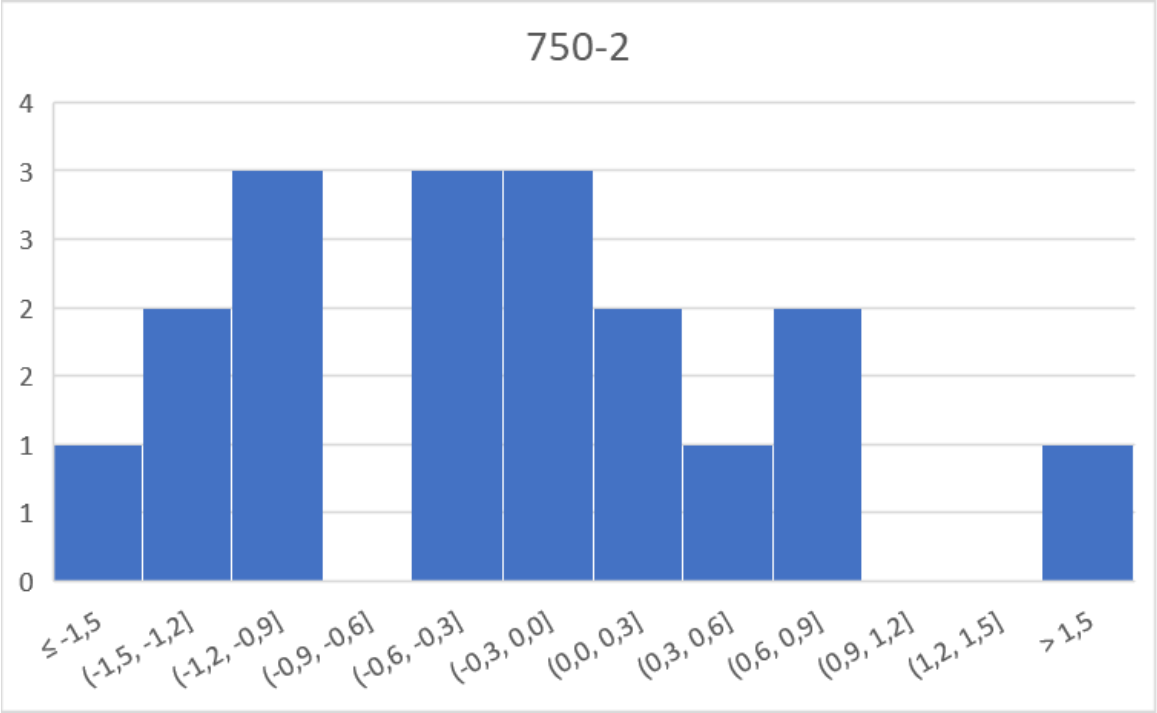


Figure 20. Histogram of difference between calculated and measured grain size of Polarit 750-2 using original parameters.

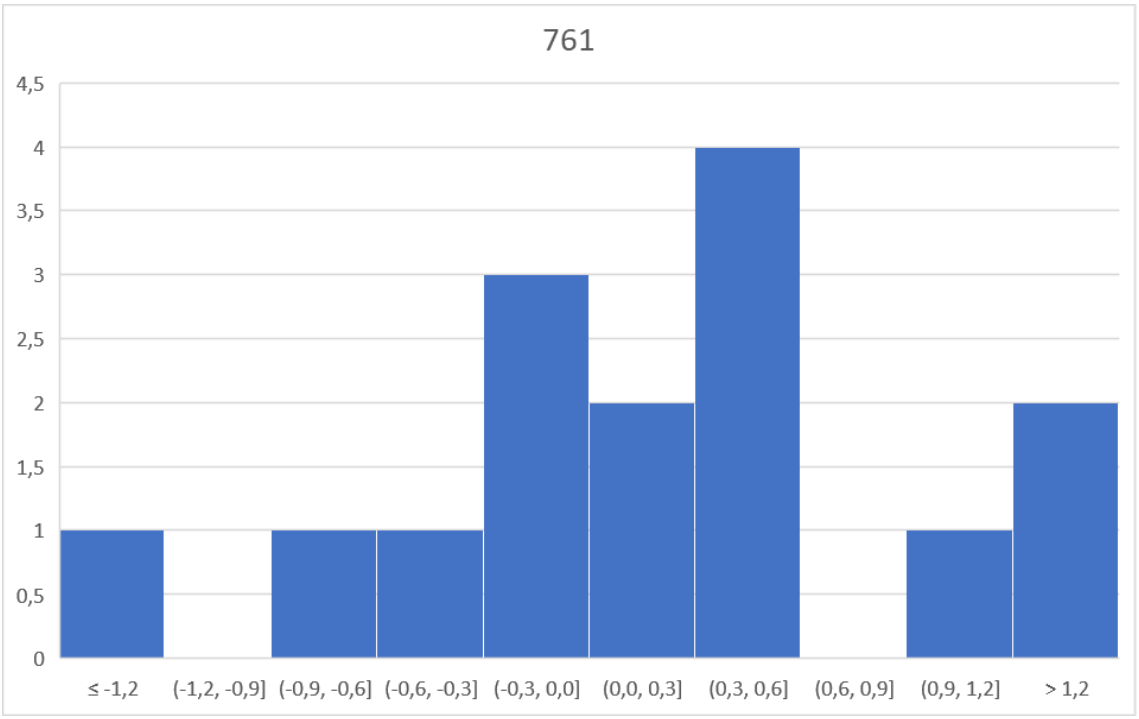


Figure 21. Histogram of difference between calculated and measured grain size of Polarit 761.

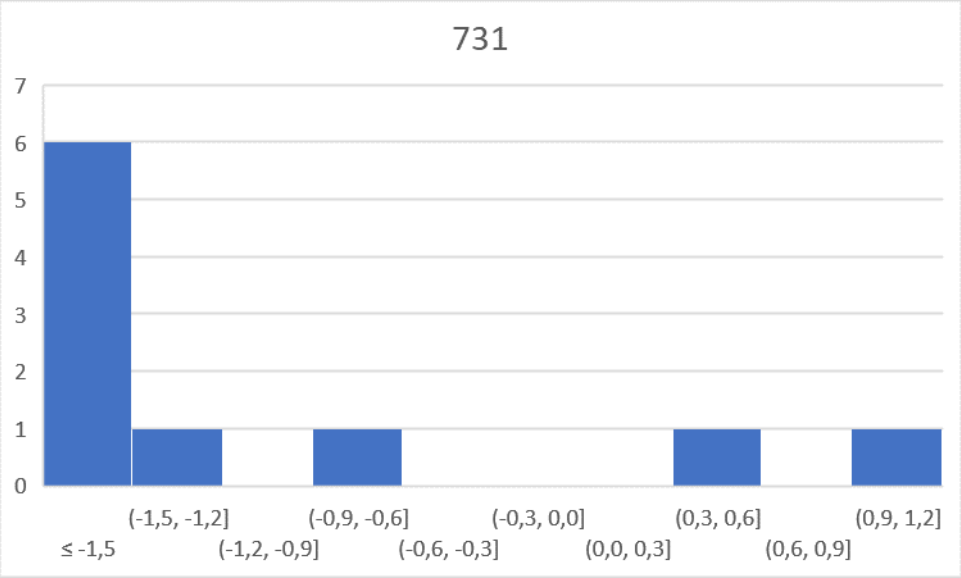


Figure 22. Histogram of difference between calculated and measured grain size of Polarit 731.

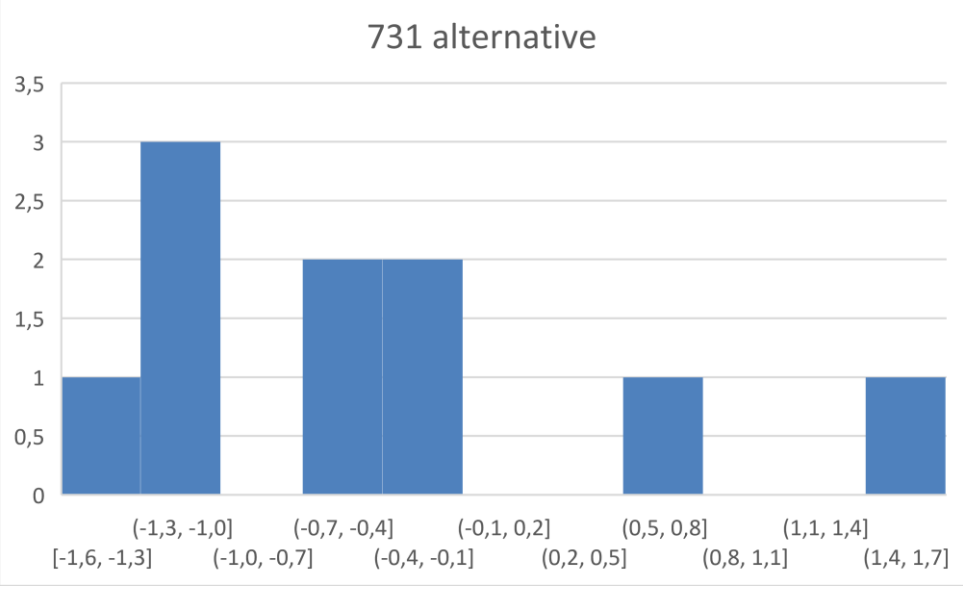


Figure 23. Histogram of difference between calculated and measured grain size of Polarit 731 using alternative parameters.